

## Experimental observations on fungal diagenesis of carbonate substrates

Kamal Kolo,<sup>1</sup> Eddy Keppens,<sup>1</sup> Alain Pr at,<sup>2</sup> and Philippe Claeys<sup>1</sup>

Received 22 March 2006; revised 10 September 2006; accepted 17 October 2006; published 27 January 2007.

[1] Carbonate substrates (dolomites and limestones) are susceptible to fungal attack that results in significant microbial diagenesis of these substrates. In a 15-day experimental study, fungi growing in Petri dishes from airborne spores attacked petrographic thin sections and chips prepared from the dolomites of Terwagne Formation (Vis an, Bocahut quarry at Avesnes-sur-Helpe, northern France) and limestones of the Morrone di Pacentro Formation (Lower Cretaceous, Italy). The analyses of the fungal material (samples of mycelia), thin sections and chips under optical microscopy, scanning electron microscope (SEM), energy dispersive X-ray (EDX), X-ray diffraction (XRD), Raman spectroscopy and stable isotopes (C and O) revealed an extensive fungally induced diagenesis. The results indicate strong diagenesis and biomineral neomorphism: neo-dolomite, glushinskite, weddellite, whewellite and possibly struvite, as well as intense substrate “de-micritization” and “micritization” with oxalates, grain bridging and cementation, open space filling, formation of intergranular and intragranular porosity, and permeability enhancement. Advanced stages of diagenesis were characterized by dissolution and replacement of original minerals by new substrates produced by fungal biomineralization. The formation of new substrates on the original attacked surfaces produced microscale stratification. Stable isotope analysis of fungal biomineralized material and of attacked and unattacked chip surfaces revealed marked differences in their isotopic signatures. The C and O isotopes of biomineralized material within the fungal mass were fractionated differently as compared to the signature measured in the original and unattacked surfaces. In sedimentary cycles, such microbially modified isotopic signature of carbonate substrates may be used to define microbial events, and consequently whether certain types of diagenesis were produced by microbial interaction. The finding of neo-dolomite formed during fungi-dolomite substrate interaction suggests the possibility of sedimentary dolomite recycling in a fungal microenvironment. The results of this experimental study confirm the significant role of fungi in reshaping carbonate substrates and forming new biominerals in the natural environment.

**Citation:** Kolo, K., E. Keppens, A. Pr at, and P. Claeys (2007), Experimental observations on fungal diagenesis of carbonate substrates, *J. Geophys. Res.*, 112, G01007, doi:10.1029/2006JG000203.

### 1. Introduction

[2] Lichenous, mycorrhizal and saprotrophic fungi interact with natural rock systems, soil and buildings (carbonates (limestone, dolomite, marble), sandstones, gypsum and granites) under a broad variety of environmental conditions [Landeweert *et al.*, 2001; Hoffland *et al.*, 2004]. This interaction results in the bioweathering of the mineral substrates, in the formation of secondary biominerals on the attacked substrates [Chen *et al.*, 2000; Burford *et al.*, 2003b; Hoffland *et al.*, 2004] and eventually in the diagenesis of the mineral substrates. This fungally induced dia-

genesis can be attributed to biochemical and biomechanical alteration induced by fungi on the rock substrates.

[3] Biochemical diagenesis involves the dissolution of the mineral substrates by organic acids (oxalate, citric, and malate) exuded in the fungal growth environment. These strong chelators and metal-binding acids [Gadd, 1999] form complexes with various metals in the mineral substrates: calcium (Ca), magnesium (Mg), manganese (Mn), Zinc (Zn), copper (Cu), aluminum (Al) and Iron (Fe) in a process of metal mobilization and immobilization that causes mineral dissolution and precipitation of new minerals [Sayer and Gadd, 1997; Gadd, 1999, 2002; Gadd *et al.*, 2002]. The minerals formed by this process are mainly Ca- Mg-oxalates (weddellite:  $\text{CaC}_2\text{O}_4 \cdot \text{H}_2\text{O}$ , whewellite:  $\text{CaC}_2\text{O}_4 \cdot 2\text{H}_2\text{O}$ , and glushinskite:  $\text{MgC}_2\text{O}_4 \cdot 2\text{H}_2\text{O}$ ), and carbonates (calcite), although a wider variety of newly formed minerals could precipitated in response to a substrate’s specific mineralogy [Burford *et al.*, 2003a, 2003b; Kolo and Claeys, 2005].

<sup>1</sup>Department of Geology, Vrije Universiteit Brussel, Brussels, Belgium.

<sup>2</sup>D partement des Sciences de la Terre et de l’Environnement, Universit  Libre de Bruxelles, Brussels, Belgium.

Fungal metabolic products (organic acids) not always contribute to the newly formed minerals. In their study on the bioweathering of a lichen encrusted granite, *Lee and Parsons* [1999] found that silica-rich layers were the only minerals precipitated by the bioweathering of the granite substrate. The common metal oxalates were not detected. According to *Sterflinger* [2000] biochemical diagenesis can also produce features such as crystal etching, grooves, and borings by fungal hyphae.

[4] Dissolution can introduce a new diagenetic rock fabric. *Burford et al.* [2003a] suggested that a diagenetic “mycogenic fabric” is formed by epilithic and endolithic fungi through the transformation of limestone and dolomite minerals. Consequently, the weathering of rocks and minerals by fungi contributes significantly to the biogeochemical cycle of chemical elements of organic or inorganic material and plays a fundamental role in soil and sediment formation.

[5] Biomechanical diagenesis is caused by fungal hyphae invasive growth and penetration of the rock surfaces [*Burford et al.*, 2003b; *Sterflinger*, 2000; *Hoffland et al.*, 2004]. Fungal appressoria, using osmotic pressure, produce sufficiently high pressure to dislodge mineral grains [*Sterflinger*, 2000, *Burford et al.*, 2003b]. Fungal biomechanical forces do not seem to play a major role in mineral diagenesis, but rather facilitate the biochemical dissolution by rock disintegration, thus increasing the surface area exposed to organic acids.

[6] The depth and extension of fungal attack on the mineral substrate, although controlled by various factors (fungi type, nutrient availability, porosity, mineral composition, temperature and light), is on the order of a few millimeters for lichenous fungi [*Chen et al.*, 2000] interacting with carbonate or granite rocks, to hundreds of centimeters in soil mycorrhizal fungi [*Jackson et al.*, 1996; *Landeweert et al.*, 2003; *Hendricks et al.*, 2006]. While the depth of interaction with exposed rock surfaces seems limited, the mineral composition and the fabric of the attacked substrates undergo major alteration.

[7] In nature, fungal diagenesis of sediments occurs in both subaerial and aquatic environments [*Burford et al.*, 2003b; *Golubic et al.*, 2005]. Endolithic fungi bioerode corals and sediment particles [*Golubic et al.*, 1970; *Tudhope and Risk*, 1985; *Bentis et al.*, 2000; *Vogel et al.*, 2000; *Golubic et al.*, 2005]. Fungi produce desert varnish in subaerial environments by biomineralization, dissolution, metal transport and transformation of the rock substrate [*Verrecchia*, 2000; *Russ et al.*, 1996; *Arocena et al.*, 2003; *Gadd*, 1999, 2002; *Burford et al.*, 2003a, 2003b]. Lichens in their various forms, cryptoendolithic, chasmoendolithic and euendolithic, are considered as the earliest colonizers of rock surfaces on Earth [*Chen et al.*, 2000]. Fungi as a mycobiont of lichen cause diagenetic alteration of the rock substrate through a symbiotic partnership with algae, in which algae provide carbohydrates through photosynthesis while the fungi supply water and minerals. As observed by *Garvie et al.* [2000], in the Sonoran desert, the endolithic lichen *Verrucaria rubrocincta* Breuss induced the dissolution and calcite biomineralization of caliche deposits.

[8] Calcium carbonate and several types of oxalates (mainly Ca- and Mg-oxalates) form as diagenesis precipitates on fungi-rock interface of various rock types:

granite, dolomite, limestone and basaltic rocks [*Wilson et al.*, 1980; *Wilson and Bayliss*, 1987; *Garvie et al.*, 2000; *Arocena et al.*, 2003; *Kolo and Claeys*, 2005]. In a case study, *Verrecchia et al.* [1993] suggested that Ca-oxalates biomineralized by fungi, contributed to the formation of calcrete deposits through their transformation into CaCO<sub>3</sub>. Gypsum (CaSO<sub>4</sub>·2H<sub>2</sub>O) was also effectively solubilized in vitro by both *Aspergillus niger* and *Serpula himantoides* [*Gharieb et al.*, 1998]. Fungal hyphae produced specific “tunneling” in feldspar grains in a boreal podzol [*Hoffland et al.*, 2002].

[9] Fungal diagenesis can be economically and aesthetically significant, when fungi attack carbonate monuments and buildings [*Hoffland et al.*, 2004], causing dissolution by their exuded organic acids. Through this capacity, fungi have been implicated in the biodeterioration and degradation of cultural heritage monuments and edifices by causing pitting, exfoliation, and discoloration [*Sterflinger*, 2000; *Warscheid and Braams*, 2000; *Rios and Ascaso*, 2005].

[10] Fungal interaction with sediments and rock substrates is often examined only in the context of biomineralization and biodegradation as the main aspects of bioweathering processes. Literature is rather scarce on fungal diagenesis of sediments involving processes such as cementation and cement typification, neomorphism and mineral replacement, dissolution fabrics, micritization and demicritization, stratification, mineral grain size, porosity and permeability reduction or enhancement, and stable isotopes fractionation. In sedimentary environments, these processes are very slow and extend over hundreds to millions of years compared to the relatively fast, but efficient diagenetic processes induced by fungi.

[11] Through experimental study, the present work investigates the diagenetic processes induced by fungi on carbonate surfaces and presents evidence from x-ray diffraction (XRD), scanning electron microscopy-energy dispersive analysis (SEM-EDX), Raman spectroscopy and stable isotope analyses on the ability of fungi to produce, within a very short time, not only bioweathering, but also significant diagenetic features, similar to the ones produced in sedimentary environments.

## 2. Materials and Methods

### 2.1. Samples Description and Preparation

[12] The experimental work involved the observation and recording of diagenetic features induced and produced by fungal attack on the carbonate substrates of thin sections and rock chips. Standard petrographic thin sections (30 μm) and rock chips (2 × 2 × 1 cm) serving as experimental dolomitic and calcitic substrates were prepared from dolomudstones of the Terwagne Formation (Viséan, Bocahut quarry, in northern France) and limestones of the “Morrone di Pacentro” Formation (Lower Cretaceous, Italy [*Bruni*, 2003]).

[13] The Terwagne Formation (Early Viséan), about 57 m thick, is composed of metric to plurimetric parasequences of fenestral calcispherid-codiaceans-spongiostromid wackestones and bindstones with a few mollusks and ostracods. The sequences are capped by fine-grained idiotopic dolomites and collapse microbreccia with abundant sulphate pseudomorphs [*Mamet and Prétat*, 2005]. These parase-

**Table 1.** The  $\delta^{13}\text{C}$  and  $\delta^{18}\text{O}$  (PDB Values) of Biominerals Formed on Attacked Substrates and Unattacked (Original) Substrates<sup>a</sup>

Sample-157 Terwagne Fm. (France)	Extracted Biominerals Ca and Mg- Oxalates		Attacked Substrate Surfaces		Unattacked Surfaces (Original)	
	$\delta^{13}\text{C}$	$\delta^{18}\text{O}$	$\delta^{13}\text{C}$	$\delta^{18}\text{O}$	$\delta^{13}\text{C}$	$\delta^{18}\text{O}$
First batch	-4.245	-1.848	+1.986	-9.805	+2.053	-9.417
	-4.181	-1.746	N.A	N.A	+2.141	-9.377
	N.A	N.A	N.A	N.A	+2.308	-9.163
	N.A	N.A	N.A	N.A	+2.248	-9.209
Second batch	-4.252	-1.756	+1.946	-9.768	+2.075	-9.377
	N.A	N.A	N.A	N.A	+2.297	-9.440
	N.A	N.A	N.A	N.A	+2.170	-9.387
	N.A	N.A	N.A	N.A	+2.264	-9.459

<sup>a</sup>N.A: Not available (collectable material too low for analysis).

quences record the transition from very shallow subtidal restricted lagoons with supratidal cryptalgal/stromatolitic laminites to semi- evaporitic sebkhas.

[14] The Morrone di Pacentro Formation (Late Jurassic–Early Cretaceous) contains well-bedded lagoonal to supratidal carbonates, deposited in a quiet environment. Microfacies are composed of microporous mudstones and wackestones with poorly preserved benthic foraminifers and various algae (mainly codiaceans, dasycladaceans) and loferites with stromatolites. Laminar cryptalgal mats are commonly associated with mud cracks and are capped by paleosoils with abundant rhizoconcretions, alveolar textures and calcite microspar. Dolocretes with sulphate pseudomorphs are also present. Extensive surfaces of exposure cover fenestral mudstones and wackestones.

[15] Thin sections were prepared in duplicate to observe the fungal interaction during the course of the experiment. The dolomitic thin sections provided the Mg and Ca, required either for reaction with oxalic acid (the main fungal metabolite) or for possible uptake by fungi during the growth process or both. The fungal growth medium consisted of protein-carbohydrate solids and a sugar solution. The solids formed attachment and launching platforms for growing fungal hyphae.

## 2.2. Methods

[16] Thin sections were placed separately in Petri dishes (90 mm diameter) with 20 g of the growth medium. The growth medium solids surrounded the thin sections but did not touch their surfaces. Ten ml of a sugar solution (10% dextrose and sucrose each) prepared with deionized water were added to each Petri dish, such that the sugar solution did not wet the thin section surfaces.

[17] Petri dishes (90 mm diameter) containing four rock chips (2 × 2 × 1 cm) of the same sample were placed with the growth media in a fume hood under the same laboratory conditions as above. All Petri dishes were numbered and dated. The experiment occurred under free air circulation and variable light, pH, and room temperature (20~25°C) to mimic natural field conditions. Throughout the experiment, the samples were kept stationary, even when sampled for analyses. When moisture content in the Petri dishes was low, the samples were sprayed with deionized water.

[18] Fungal growth on the growth media was expected to occur naturally from airborne fungal spores. Observations were recorded every 48 hours. The extracellular polymeric substance (EPS) layer formed on the dolomitic and calcitic substrates was examined under an optical microscope for biomineralization products. Slides for microscopic analysis were prepared without mounting material, cover glass or staining to ensure a true image of fungal-mineral interaction. These same slides were also used for SEM and EDX analyses of the mineral phases associated with the fungal mass. The newly formed minerals embedded in the fungal mass and EPS layer were extracted by digesting the organic mass in 30% H<sub>2</sub>O<sub>2</sub> at 30°C for 60 minutes in a magnetic stirrer, followed by successive settling, decantation and washings with deionized water. The crystal residue was removed from the liquid by suction and mounted on glass slides.

[19] Two collections of samples were taken from the four rock chips of sample-157 (Terwagne Formation) for stable isotope analysis. Each collection contained three sets of samples. The first set represented the fungal mass with EPS layer and embedded biominerals. The second contained material collected from the upper surfaces of the attacked chips, sampled with a micro-drill penetrating ~ 0.5 mm into the sampled chip surfaces. The third set (rock powder) was obtained before the experiment from the lower surfaces of the rock chips, also using a micro-drill. This latter set of samples represents the original bulk isotopic signature of sample-157. The upper and lower surfaces were thoroughly sampled to ensure a good representation of the sample surfaces. The two collections were named Batch 1 and Batch 2 respectively. All of the collected samples were oven dried at 50°C for 24 hours before isotopic analysis (Table 1).

## 2.3. Instrumentation

### 2.3.1. SEM-EDX

[20] The data pertinent to biomineral morphology, distribution, chemistry, and the relationship to fungal mass and EPS layer was acquired using a JEOL- JSM-6400 scanning electron microscope (SEM) at 20 kV and a working distance of 39 mm; the instrument was equipped with an energy dispersive x-ray (EDX) facility (Thermo-Noran Pioneer with Si-Li detector). The spectra treatment

was done with a SUN workstation, using Voyager III software. Sample coating was done with an EMITECH-Carbon evaporator K450 for carbon coating and a BALZERS BAE80 high vacuum coating system for gold and aluminum. All the images and analyses were acquired in the normal mode.

### 2.3.2. Raman Spectrometry

[21] The minerals were identified by multiple Raman spectrometry measurements on selected single crystals. The Raman spectrometer is a Dilor XY equipped with an Olympus BH2 microscope (50x objective was used simultaneously for illumination and collection) and a liquid nitrogen cooled  $1024 \times 256$  CCD-3000 detector. The excitation source is a Coherent Innova 70C Argon/Krypton mixed gas laser (excitation at 514.5 nm, laser power at 25 mW). Integration time ranged from a few seconds up to a maximum of 1 minute per spectral domain. Baseline subtraction and smoothing were carried out on the spectra to improve readability. The crystals to be analyzed were identified using a video camera attached to the microscope.

### 2.3.3. X-Ray Diffraction

[22] A Siemens GADDS-MDS (Micro Diffraction System) instrument was used for mineral identification in clusters within the fungal mass, EPS layer, thin section surfaces and extracted crystals. The extracted crystals and selected parts of the fungal mass and EPS layer were mounted on glass slides after microscopic examination of their mineral content and richness. With the micro-video camera on the GADDS-MDS system, it was possible to target specific parts on the fungal mass, EPS layer and thin sections, lowering in this way the background signal.

### 2.3.4. Stable Isotope Analysis

[23] Carbon and oxygen isotopes were analyzed using a dual outlet Finnegan Mat delta E Isotope Ratio Mass Spectrometer on  $\text{CO}_2$  obtained from the dissolution of carbonate samples in  $\geq 100\%$  orthophosphoric acid at  $25^\circ\text{C}$  under vacuum and cryogenic separation from the reaction mixture, using the procedure adopted by *McCrea* [1950]. Carbon and oxygen isotope ratios are reported in delta notation, expressed in per mille relative to V-PDB and corrected, following procedures modified from *Craig* [1957] and calibrated with NBS-19 [*Caplan*, 1994]. Reproducibility, determined by replicate analyses of laboratory standards is better than  $0.05\%$  for  $\delta\text{C}$  and better than  $0.07\%$  for  $\delta\text{O}$  at the  $2\sigma$  level.

## 3. Results

### 3.1. Fungal Growth

[24] After 48 hours, fine whitish and translucent fungal hyphae were observed on the solid protein/carbohydrate growth media in all Petri dishes. By the fourth day, the fungal hyphae filled the entire dish space and gradually displayed a darker color. Extensive sporulation started within the first week. The growing fungi were identified as *Rhizopus* and *Mucor* (*A. Gorbushina*, personal communication, 2005).

[25] Where fungi grew in the Petri dishes, a thick layer (3–4 mm), consisting of mucilaginous material and fungal mass, developed over the thin sections and rock chips. The fungi developed attachment rhizoids on the mineral phase and within the mucilaginous substrate. This mucilaginous

material is the extracellular polysaccharide (EPS) produced by fungal bioactivity [*Jones*, 1994; *Gadd*, 1999; *Sterflinger*, 2000; *Verrecchia*, 2000].

[26] Daily microscopic observation of the thin section duplicates revealed that the biomineralization on the hyphae started after 10 days, when fungal filaments began to display crystals attached to the hyphal sheath. The newly formed minerals decreased in abundance upward along the fungal hyphae. The lower parts of the hyphae attached to the rock surface and passing through the mucilaginous substrate showed a higher concentration of newly formed biominerals. Filament parts not attached to rock surfaces did not display any biomineral formation as free crystals within the fungal mass or as attachments to fungal sheaths.

### 3.2. Fungal Interaction With the Substrates

[27] After the second week, intense formation of biominerals with clear morphologies was observed on the fungal hyphae. The fungi attacking the Viséan dolomitic substrate formed tetragonal bipyramidal, prismatic and rhombic crystals of various size and frequency rates, in the form of single, pairs, or clusters of crystals, attached to fungal hyphae. They also formed crystal envelopes, completely encrusting the fungal filaments. The fungi from the Cretaceous limestone substrate of Morrone di Pacentro Formation also produced singles, pairs or aggregates of tetragonal bipyramidal crystals, attached to the fungal filaments. The intense biomineralization produced hyphal sheaths that were completely engulfed in these packed crystals, forming an external mineral cover on the filaments. A rich biomineral precipitate not bound to fungal filaments formed on both groups of thin section substrates (dolomitic and calcitic). Under the microscope fresh and untreated specimens from the EPS layers and from the fungal mass overlying the thin sections displayed a rich array of biominerals, crosscut by the fungal network. Specimens of EPS layers and fungal mass not in direct contact with the thin section surfaces did not show any biomineral content.

[28] Total destruction and “digestion” of the exposed surfaces of the duplicate thin sections was observed after 15 days of experimenting. Fresh substrates were formed with new minerals replacing the original dolomite and calcite. After 15 days, all thin sections were carefully removed from the Petri dishes, oven dried at  $30^\circ\text{C}$  for 24 hours and subjected to optical, SEM-EDX, XRD and Raman analyses. The rock chips, EPS layer, and fungal mass were sampled for isotope analysis.

### 3.3. Observed Diagenetic Processes

#### 3.3.1. Substrate Dissolution

[29] The carbonate substrates showed progressive dissolution that culminated in a few cases in the total disappearance of the substrate. Along the thin sections, several dissolution zones (zones A–D, Figure 1a) developed reflecting different levels of dissolution intensity: severe dissolution in zone A, medium low in zones B and C and no dissolution in zone D. The dissolution front advanced from zone A at the edge of the thin section toward zone D. A dense infill by new biominerals in the dissolution space also occurred (Figure 1a, inset). The dissolution created several levels of thickness, each of a few microns (Figures 1a and 1b). In the most severely attacked and

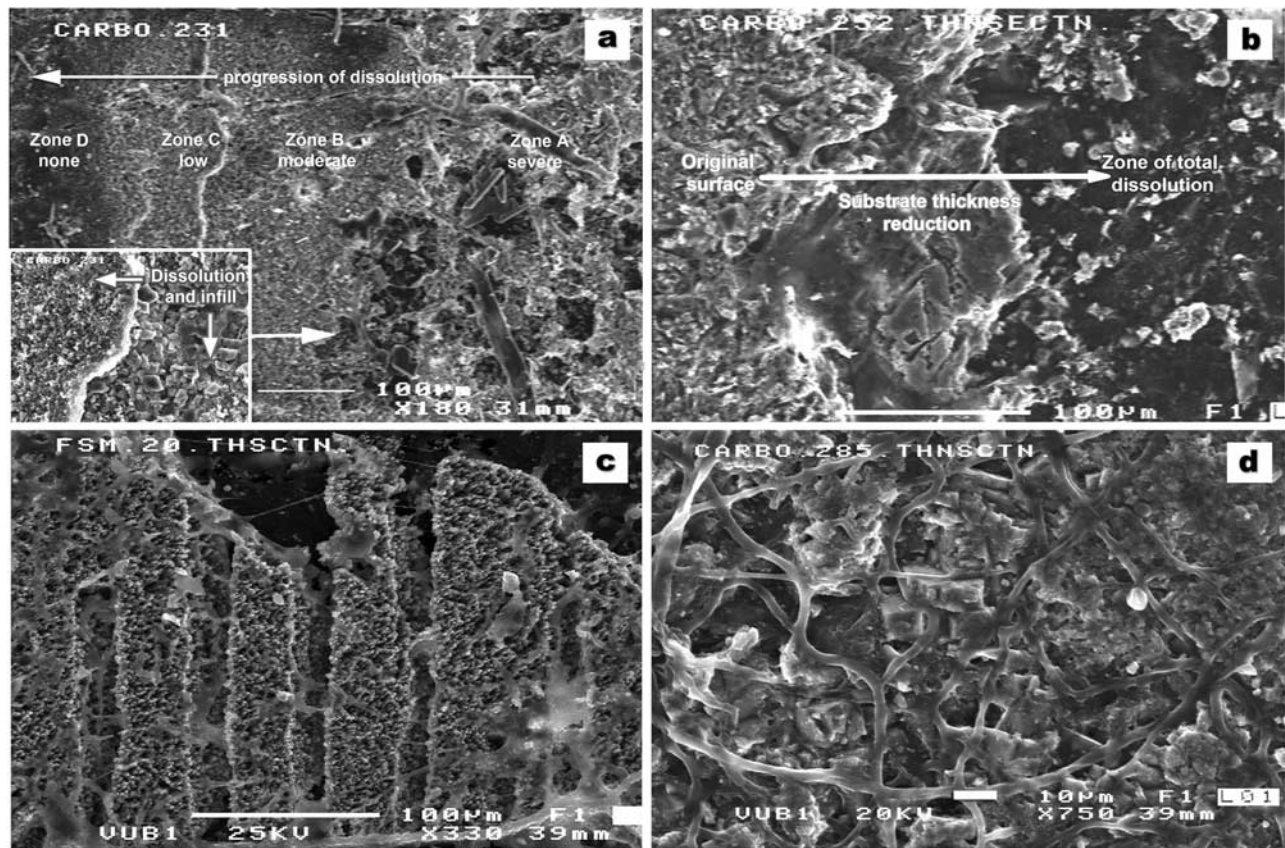


**Figure 1.** Fungal attack on carbonate substrates. (a) Four zones produced by progressive fungal dissolution of a dolomitic substrate. The zones range from severe to no dissolution. The direction of dissolution progression indicates the advancement of the ‘dissolution front’ which is also the direction of extension of the EPS layer. The inset figure details the resulting difference in thickness between two zones: A and B and also the infilling by new biominerals. (b) Dolomitic substrate showing a zone of total dissolution on the thin section. The black background is the slide’s glass. Two other zones appear severely and moderately attacked and reveal the resulting thickness difference. (c) Differential dissolution induced by fungi along lines of substrate weakness. The cleavage planes on calcite crystals show straight and deep dissolution compared to the rest of the thin section. The pitting dissolution marks the entire thin section and produced columnar structures. It indicates removal of finer material. Notice the fungal hyphae network crisscrossing the surface. (d) A network of fungal hyphae penetrating the dolomitic substrate and circumventing the grains’ boundaries. The hyphae have created dissolution paths around the more susceptible grain boundaries. Notice how the level of hyphae is below the surface of the attacked substrate, indicating more pronounced dissolution along penetration paths of hyphae. These hyphae, when biomineralized, act like binding bridges and cement of the grains. Figures 1a, 1b, and 1d are dolomitic thin sections, Terwagne Fm., France. Figure 1c is a limestone thin section, Morrone di Pacentro Fm. All are SEM photomicrographs; bar scale = 100, 100, 100 and 10  $\mu\text{m}$ , respectively.

dissolved zones, the glass of the thin section was exposed, indicating total dissolution (Figure 1b).

[30] Mineral cleavage planes, preferentially dissolved, showed a straight and deeper dissolution pattern than the rest of the substrate (Figure 1c). The surface was heavily pitted, owing to preferential removal of finer matrix material. A new microscopic columnar texture was formed owing to this preferential dissolution. The different parts of the substrate were connected by biomineralized (white spots on the filaments) fungal hyphae (Figure 1c).

### 3.3.2. Grain Boundaries Selectivity

[31] A specific dissolution-penetration pattern was formed by fungal hyphae. In Figure 1d, the hyphae (grey filaments) penetrated the attacked substrates along grain

boundaries to form a network within the newly created space between the grains. Grain boundaries showed another specific feature of differential fungal attack that involved dissolution and biomineral precipitation. In several substrates, fungi had preferentially precipitated Ca-oxalate on grain boundaries, thus creating typical honeycomb structures (Figure 2a, inset). The deeply “bored” mineral grains formed chambers with standing walls (Figures 2a and 2b). While the deposition of biominerals preferentially occurred on grain boundaries, the bored chambers remained empty or with minor infilling of new biominerals. Interestingly, the mineral deposit on grain boundaries was quite thin, not exceeding a few microns ( $\approx 10 \mu\text{m}$ ), while the crystal size of the biominerals was only  $\approx 1 \mu\text{m}$  (Figures 2a, inset, and 2b).

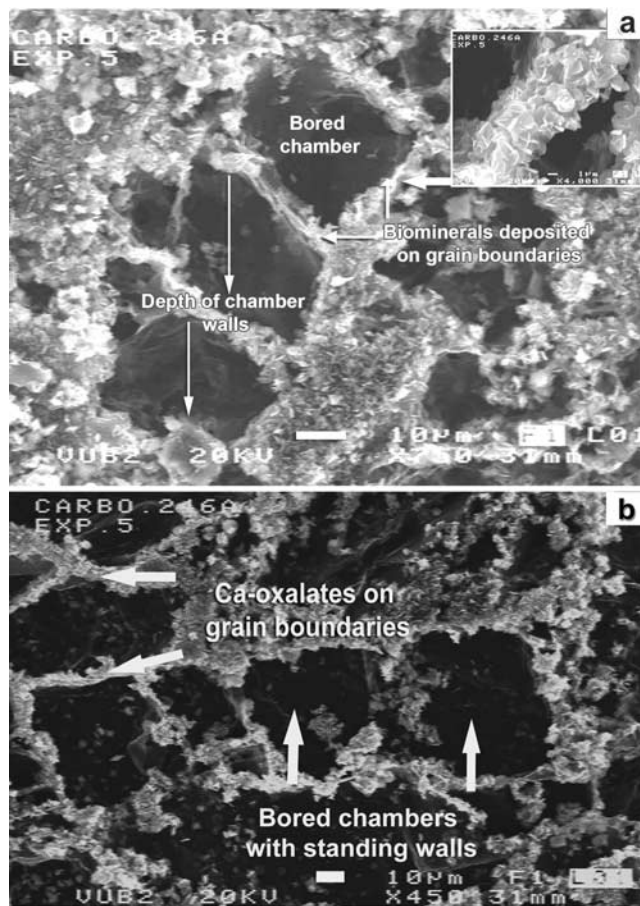


**Figure 2.** Selective deposition of biominerals on grain boundaries by fungi. (a, b) SEM photomicrographs showing the preferential deposition of fungally produced biominerals on the dolomite grain boundaries. The inset image (in Figure 2a) details this fine-line selective deposition. The crystals themselves are selectively deeply bored by fungal attack that created chambers with standing walls, intragranular and mouldic porosity at the same time. The empty chambers definitely indicate that grain boundaries are places of choice for biomineral deposition. Later, the whole image developed into full honeycomb structure. Ghost structure of the rhombic form of dolomite crystals is also formed. All are dolomitic thin sections, Terwagne Fm., France; bar scale = 10  $\mu\text{m}$ .

Progression of selective dissolution-deposition on grain boundaries produced true alveolar structures (Figures 3a and 3b). A single dolomite crystal showed a peculiar diagonal dissolution and precipitation pattern. The grain was only partially dissolved, but the pattern stood diagonal to the rhombic form of the crystals (Figure 3c).

### 3.3.3. Neo-Mineral Formation and Biomineralization

#### 3.3.3.1. Ca- and Mg- Biominerals

[32] Newly formed Ca- and Mg- biominerals were identified on the attacked substrates. On the calcitic substrates, only biominerals consisting of Ca were found. On the dolomitic substrates, both Ca- and Mg- biomineral groups coexisted, along with a third biomineral group composed of both Ca and Mg (Figure 8b in section 3.3.3.4). The latter

produced an EDX signature and displayed the rhombic crystal form of natural dolomite.

[33] The EDX spectrum of the first group represented by prismatic bipyramidal crystal habits revealed a Ca, C, and O (Figure 4a) composition. These crystals formed the bulk of the newly precipitated crystals on the thin section surfaces. X-ray diffraction analysis (Figure 4b) confirmed the presence of Ca-oxalates (weddellite and whewellite) in the first group of minerals. The second group with lamellar spindle shapes, which appeared under optical microscope as striations produced an Mg, C, and O composition (Figure 5a). The lamellae seem to have originated from a central longitudinal axis. The second group displayed an XRD pattern characteristic of glushinskite ( $\text{MgC}_2\text{O}_4 \cdot 2\text{H}_2\text{O}$ ), the  $\beta$ -magnesium oxalate dihydrate (Figures 5a and 5b) [Kolo and Claeys, 2005].

#### 3.3.3.2. Raman Signature of Ca- and Mg- Biominerals

[34] Raman spectroscopic analyses of the extracted crystals produced typical spectra for the minerals weddellite (Figure 6) and glushinskite (Figure 7). Whewellite was not found, even though its presence was indicated by the XRD analysis. The Raman spectra (Figure 6) of a selected single large crystal showed an intense band at  $1476\text{ cm}^{-1}$  and a low band at  $1417\text{ cm}^{-1}$  corresponding to the symmetric C-O stretching vibration, which is cation-mineral dependant [Frost and Weier, 2003a, 2003b]. A low band corresponding to the antisymmetric stretching region appeared at  $1629\text{ cm}^{-1}$  and a high band in the  $\nu(\text{C}=\text{C})$  stretching region at  $913\text{ cm}^{-1}$ . A low band was observed in the C=C-O bending region at  $502\text{ cm}^{-1}$ . The 193, 225,  $234\text{ cm}^{-1}$  triplet appeared in the low wave number region. These bands corresponded to the OMO ring bending mode. In the hydroxyl-stretching region, a low broad band appeared at  $3462\text{ cm}^{-1}$ . These values are in good agreement with the published Raman data for weddellite [ $\text{CaC}_2\text{O}_4 \cdot 2\text{H}_2\text{O}$ ] [Frost and Weier, 2003a]. Whewellite [ $\text{CaC}_2\text{O}_4 \cdot \text{H}_2\text{O}$ ] was not identified.

[35] The Raman analysis of the large, foliated, spindle shaped and Mg-bearing crystals produced a different signature (Figure 7). In the symmetric C-O stretching region at  $1473\text{ cm}^{-1}$  an intense band appeared that is associated with a shoulder band at  $1445\text{ cm}^{-1}$ . Other bands appeared at 3369 (obscured by the high intensity of the  $1473\text{ cm}^{-1}$  band), 1720, 1638, 920, 584, 528, 272, 232 and  $124\text{ cm}^{-1}$ . These bands are in good agreement with published data [Frost and Weier, 2003a, 2003b, 2004; Frost et al., 2004] and are assigned here to the magnesium oxalate mineral glushinskite [Kolo and Claeys, 2005]. All other measurements on similar crystals produced relatively high intensities with good resolution in the low and high wave number regions.

#### 3.3.3.3. Mg-P Biominerals

[36] The third group of biominerals with Mg-P (possibly struvite:  $(\text{NH}_4)\text{Mg}(\text{PO}_4) \cdot 6\text{H}_2\text{O}$ ) was also formed during the interaction with dolomite substrate. Figure 5b with the EDX inset shows the large size ( $\approx 500\text{ }\mu\text{m}$ ) Mg-P crystals arranged in a shape of “desert flower”.

#### 3.3.3.4. Mg-Ca Biominerals

[37] The fourth group is an Mg-Ca biomineral, and is of specific importance. Their crystal form displays high similarity to the crystal habit of natural dolomite (Figures 8a, 8b, and 8c). This similarity is also supported by their EDX and XRD patterns (Figures 9a, 9b, 9c, 9d and 9e).

Figure 8a shows the rhombic crystals in a structure similar to saddle structure known for dolomite. This fourth group corresponds to microbial dolomite precipitated during the fungal-dolomite substrate interaction.

### 3.3.4. “Demicritization”

[38] “Demicritization” is defined here as a process through which the original micritic material of the carbonate substrate is removed by fungal dissolution, which leaves the much larger dolomite or calcite crystals as isolated islands surrounded by emptied space, at least in the early stage of dissolution. Figure 10a shows a demicritized zone on a dolomitic substrate where the fine-grained

material (cement) filling the space between dolomite crystals has been removed, leaving in place the more resistant dolomite crystals. In the same area, the newly formed minerals replaced the old material that was consumed through fungal dissolution and chemical element uptake. The crystal size of the new biomineral infill is between 1 and 3  $\mu\text{m}$ . The micrite-size new biominerals are composed of Ca-oxalates and possibly Mg-oxalates. According to *Verrecchia* [2000] it is only through further diagenesis that this new biogenic “micrite” is transformed into true cryptocrystalline calcite. The current use of the term “micritization” is thus in anticipation of such diagenetic transformation.

### 3.3.5. “Micritization”

[39] “Micritization” is characterized by the precipitation of biominerals of small grain size ( $\sim 1 \mu\text{m}$ ) in the porous space between grains previously created by the demicritization process (Figures 10a and 10b), and on the original substrate crystals (Figure 10c). By filling and connecting the grains, the new biominerals form a new cementing phase. Figure 10d (and inset) shows the complete substrate micritization with newly precipitated biominerals. In fact, a new substrate (size =  $\sim 1 \mu\text{m}$ ) composed of Ca-oxalates, has been formed.

### 3.3.6. Grain-to-Grain Bridging

[40] The fine-grained material (Ca-oxalates) precipitating in between and on the boundaries of the larger crystals created a mineral bridge, connecting the grains (Figures 10a, 10b, 10c and 11a). The substrate matrix in Figure 11a was removed (demicritized) and a new process of “micritization” started, with chemical precipitation of micron size ( $\sim 1 \mu\text{m}$ ) material (Ca-oxalates), including a densely biomineralized fungal hyphae as bridging material. The tip of the bridge not only touched the dolomite crystal face, but was in actual fact perfectly welded to it, making a natural

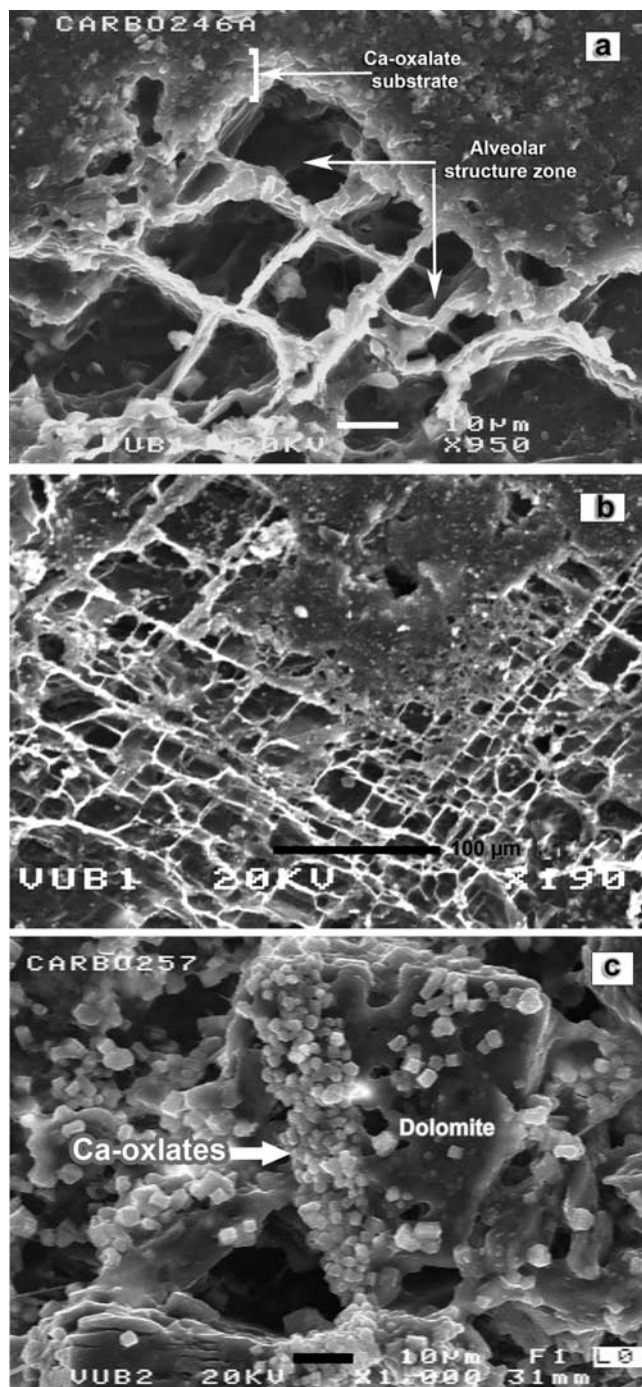


**Figure 3.** Formation of alveolar-honeycomb structures and diagonal crystal dissolution and replacement. (a) Formation of alveolar-honeycomb structures by fungal interaction with dolomitic substrates. The chambers are deep and empty while the separating walls are topped by biominerals (white crystals). Here the biomineral deposition on the grain boundaries is sharper and a clear layer of Ca-oxalate substrate has formed. The chambers form mouldic porosity after the dissolved dolomite grains. (b) Extensive formation of honeycomb-alveolar structures making two or three levels. The walls are separated by straight and intersecting lines that make the shape of a rhomb. These inherited forms could form ghost structures when filled by sediment or biominerals. (c) A single dolomite crystal in a dissolved substrate background. The crystal shows partial diagonal dissolution and many intragranular pores created through fungal attack. On the line of dissolution, biomineral is observed replacing the dolomite. Very fine-grained ( $1 \mu\text{m}$ ) biominerals are deposited on the surface of the dolomite crystal; these indicate a process of grain replacement and micritization by biominerals. Figures 3a, 3b, and 3c are SEM photomicrographs, dolomitic thin sections, Terwagne Fm. France; bar scale = 10, 100 and  $10 \mu\text{m}$ , respectively.

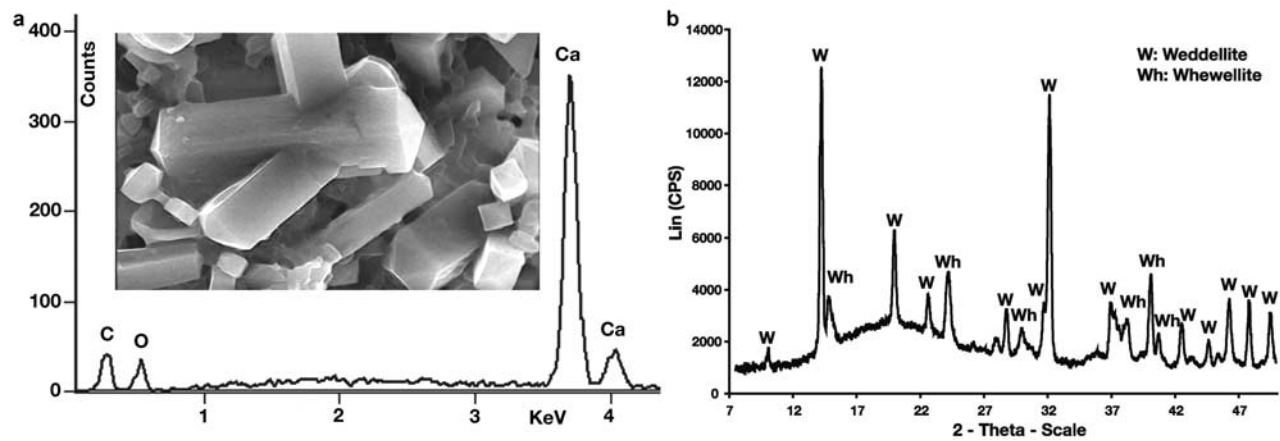


**Figure 4.** (a) Energy dispersive X-ray (EDX) analysis of prismatic and bipyramidal crystals (inserted figure) showing high calcium content with C and O. These biomineralized crystals making the fine background proved to be Ca-oxalates: weddellite and whewellite. These two biominerals were formed on both types of substrates: calcitic and dolomitic. (b) XRD analysis of biominerals formed on the calcitic substrate. The only identified minerals are Ca-oxalates: weddellite and whewellite. The formation of only these two biominerals indicates a control by the substrate chemistry ( $\text{CaCO}_3$ ).

extension. The inset in Figure 11a further shows such functions of fungal hyphae.

### 3.3.7. Cementation

[41] Cementation (more precisely recementation) of original grains in the fungally demicritized substrates is related to the new micritization process. In Figures 10a, 10b, 10c, and 11a), the grain-to-grain bridging was either an initial stage of cementation process (Figures 10c and 11a) or a well-advanced one (Figures 10a and 10b). Figure 11b shows typical and complete cementation of substrate crystals with well-developed cement suture lines between dolomite crystals.

### 3.3.8. Replacement

[42] Although compared to real field conditions, the time frame of the experiment was short, fungal interaction with the carbonate substrates did produce, at a micrometric scale, clear diagenetic replacement of original crystals by newly formed minerals. Figure 12 shows a natural 3-D pseudomorph of a calcite crystal that appears to have been replaced by the newly formed minerals (Ca-oxalates). The new Ca-oxalates minerals inherited the rhombic form of the calcite crystals. The new biomineral crystals ( $3\text{--}4\ \mu\text{m}$ ) occur in straight lines along the original margins and surfaces of the calcite crystal, where  $\text{Ca}^{2+}$  was available. The upper

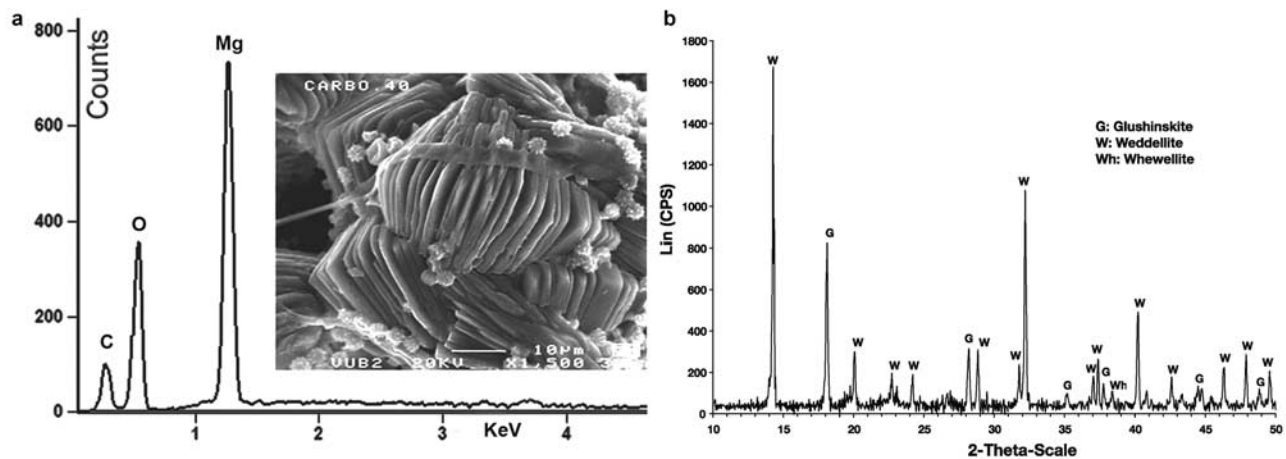


**Figure 5a.** (a) Energy dispersive X-ray (EDX) analysis of foliated and spindle shaped crystals (inserted figure) showing high Mg composition. These crystals proved to be the mineral glushinskite and formed only on the dolomitic substrates, which indicated a control by the substrate chemistry [ $\text{CaMg}(\text{CO}_3)_2$ ]. (b) XRD analysis of mineral neoformation. The identified minerals are Ca-oxalates: weddellite and whewellite as the main phase. Glushinskite appears in the background. These two biomineral groups coformed on the dolomitic substrates only.

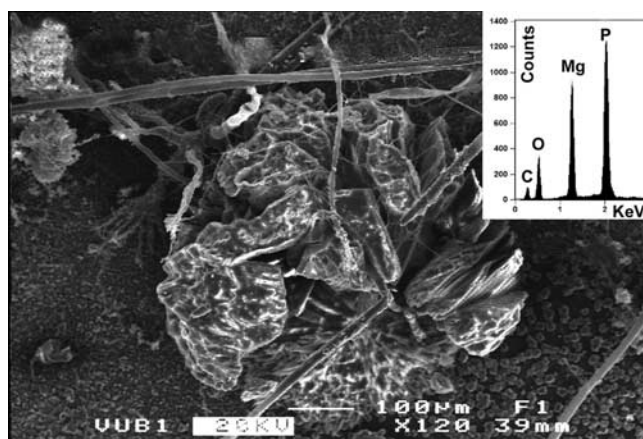


**Figure 5b.** SEM photomicrograph and EDX spectrum (inset figure) of large crystals of an Mg-P biomineral. The crystal shape, large size, and chemical composition suggest the biomineral struvite. This biomineral group was only found on dolomitic substrates, indicating a control by the substrate's chemistry.

crystal face shows a slight depression. The side margins of the crystal are higher, relative to the upper face. This suggests a simultaneous dissolution-replacement process with faster rates at larger crystal surfaces.

### 3.3.9. Open-Space Filling, Porosity, Permeability, and Grain Size

[43] Open-space filling occurred in the original pore space of the substrates (fractures, intergranular porosity) as well as in the newly formed pore space (intergranular and intragranular) produced by fungal dissolution and demicritization. Figure 13a shows a natural fracture on dolomitic substrate being filled with the newly formed biominerals (oxalates). The middle part of the fracture is nearly full and shows the same texture as the rest of the substrate surface, where extensive deposition of biominerals

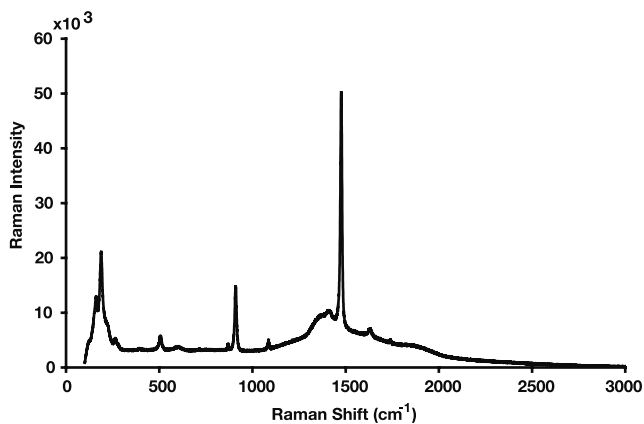


**Figure 6.** Raman spectrum of prismatic bipyramidal crystals extracted from fungal mass attacking dolomitic substrate. The spectrum obtained from single crystal analysis was cross-checked by repeated measurements on several other crystals. The spectrum is typical for weddellite.

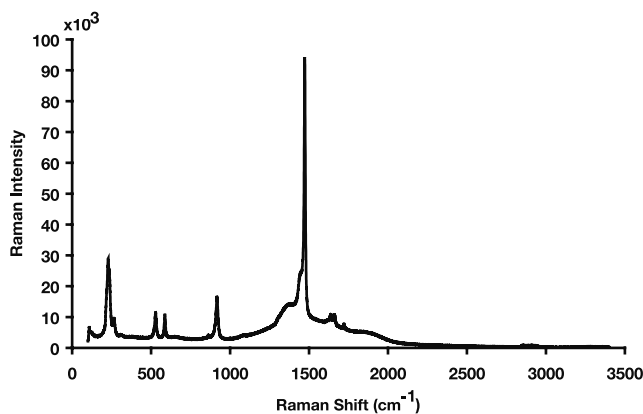


**Figure 7.** Raman spectrum of lamellar and spindle shaped crystals extracted from fungal mass attacking dolomitic substrate. Raman analysis identified these crystals (after EDX assertion of their high Mg content) as the Mg-oxalate glushinskite. The crystals produced a typical glushinskite spectrum.

has occurred. The filling of the intergranular porosity occurred as fringing cement lining the inner contour of the pore as well as partially littering the pore (Figure 13b). Secondary intragranular porosity created by fungal attack on substrate grains is filled by the biominerals produced by the fungi. Figure 13c shows a dolomite crystal with secondary intragranular porosity that is refilled with newly precipitated biominerals. The biomineral crystals are of micrometric size ( $<1 \mu\text{m}$ ) and are clustered in the pore ( $>10 \mu\text{m}$ ). In contrast to the prismatic, very small crystal size of these intragranular biominerals, the external biominerals, precipitated on the surface of the same dolomite crystal, are much larger ( $2\text{--}5 \mu\text{m}$ ) and are rhombic in shape.

[44] Some aspects of the original rock textural fabric are retained as mouldic porosity. The crystal rhombic shape, dolomite or calcite, is preserved as moulds of crystal sides. The honeycomb structures previously mentioned (Figures 2 and 3) are a good representation of mouldic porosity where the crystal contour is preserved by selective biomineral deposition on crystal boundaries while the boring of inner crystal body creates the pore space. Permeability was apparently enhanced as dissolution by the fungi created new pore space and increased the connectivity of these pores. No measurements are available to this point on the impact of fungal dissolution on both porosity and permeability, but visual evaluation suggests that the increase might be important.

### 3.3.10. Concentric Zonation Structures

[45] In Figure 14, several polygonal crystals of Ca-oxalates ( $4\text{--}5 \mu\text{m}$ ) display a concentric structure and zonation. Four successive, equidistant growth zones are visible. Fungal spores occupy the central oval-rectangular depression that also appears to have been the nucleation site (Figure 14, inset). The size of the central depression matches the size of the fungal spores involved in nucleation.

### 3.3.11. Stable Isotope Results

[46] The fungal interaction with the carbonate substrate produced a measurable change in the C and O isotope

signatures of the substrate surface. The minerals that were formed through the interaction had a different isotopic composition from that of the original substrate (Table 1). The unique isotopic signature of the new minerals indicates either the presence of a micrometric layer of the newly deposited biominerals or their fine-scale incorporation within the original substrate, resulting in a averaged bulk isotopic signature.

[47] Table 1 shows that isotopic fractionation has occurred, especially between the newly formed minerals and the unattacked surfaces. The differences in isotopic

compositions reflect the strong effect of organically incorporated  $^{13}\text{C}$  and  $^{18}\text{O}$ . The source of the carbon and oxygen in the newly formed minerals is unclear. Possible sources include the substrate (dissolution of  $\text{CO}_3^{2-}$ ), the atmosphere ( $\text{CO}_2$  in solution) and the water used in the experiment. Table 2 summarizes  $\delta^{13}\text{C}$  and  $\delta^{18}\text{O}$  values obtained for the deionized and milliQ water used in the experiment and utilized by the growing fungi. Compared to these values, the newly formed minerals are  $^{13}\text{C}$  depleted and  $^{18}\text{O}$  enriched, but the attacked substrate surfaces are  $^{13}\text{C}$  enriched and  $^{18}\text{O}$  depleted. Compared to the original unattacked surfaces, the  $\delta^{13}\text{C}$  of the newly formed minerals and attacked substrates show considerable depletion while the  $\delta^{18}\text{O}$  values show enrichment.

## 4. Discussion

### 4.1. Fungally Induced Dissolution

[48] The metal-binding capacity of fungal organic acids (oxalic, citric and malate) with the presence of hydrogen ions causes substrate mineral hydrolysis and mineral neoformation by metal-acid complexation [Chen *et al.*, 2000, Hoffland *et al.*, 2004]. The action of these strong acids is combined with the action of fungal respiratory  $\text{CO}_2$ , which generates carbonic acid in the growth environment. In the present study, it is suggested that the combined action of these two acid groups produced the dissolution pattern observed on the dolomitic and calcitic substrates (Figures 1, 2, and 3). The several dissolution levels observed on the dolomitic substrate (Figures 1a and 1b) are indicative of a progressive dissolution process that took place in the direction of fungal attack as well as of EPS layer growth on the thin section. The depth of dissolution reflects a time factor. The more severely altered parts indicate longer exposure time to fungal attack (Figures 1a–1d). Given equal experimental conditions, the two substrate types did not produce similar dissolution-related features.

### 4.2. Formation of Honeycomb-Alveolar Structures

[49] Honeycomb-alveolar structures were only produced on dolomitic substrates (Figures 2 and 3). This could be attributed to the lower solubility of the dolomite compared to the less resistant calcite [Gadd, 1999]. Differential

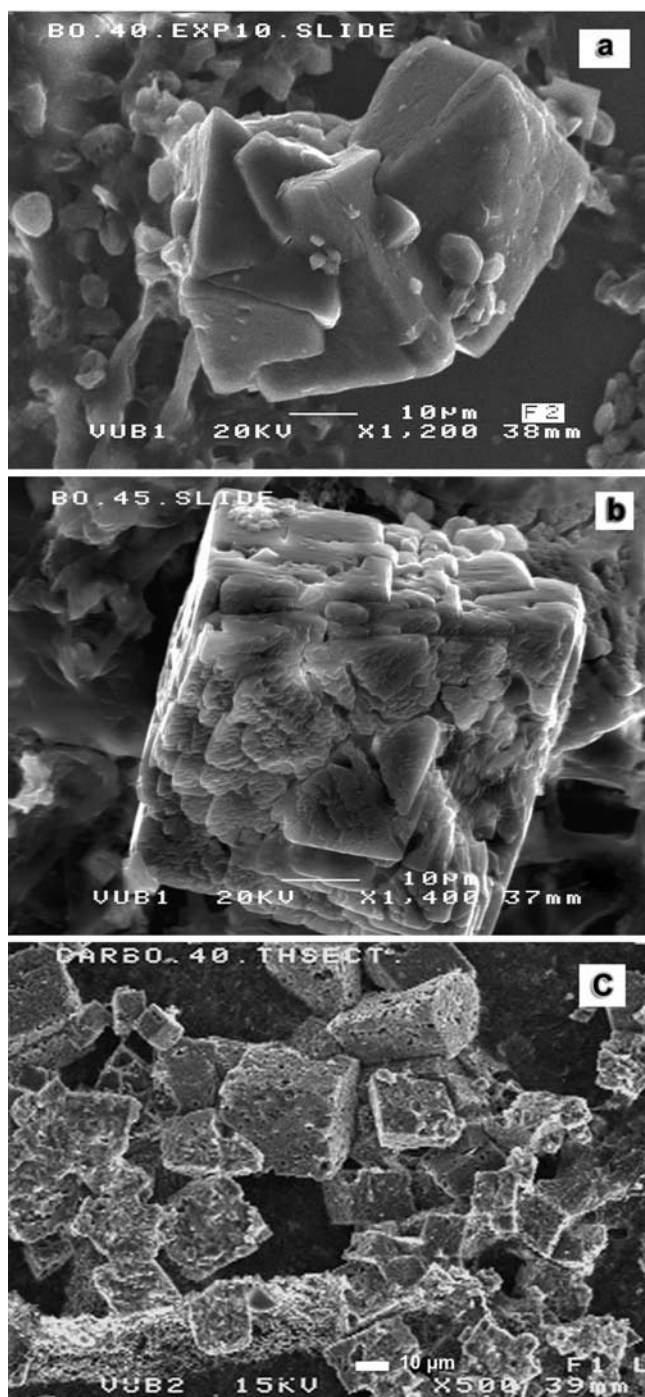


**Figure 8.** Formation of “dolomitic” biominerals. (a) SEM photomicrograph showing biominerals similar to dolomite. The crystals show multiple twinning and the form reminds of saddle structure of natural dolomite. These biomineral crystals are produced by fungal interaction with the dolomitic substrates and are composed of Mg, Ca, O and C. (b) SEM photomicrograph showing a biomineral similar to dolomite habit. The crystal shows growth features and no signs of fungal attack (Figures 8a and 8b). The EDX spectrum for these crystals is identical to natural dolomite. (c) Natural dolomite crystals extracted from the experimental substrates for EDX analysis. The EDX signature of these typical dolomites is similar to “dolomitic biominerals” formed during the experiment. All are dolomitic thin sections. Terwagne Fm. France. Bar scale = 10  $\mu\text{m}$ .

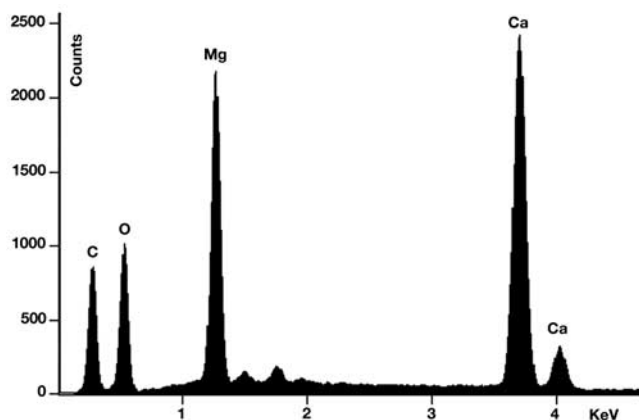


**Figure 9a.** EDX spectrum of the rhombic crystals in Figure 8a. The spectrum shows the Mg and Ca composition of the crystals. Compared to the EDX spectrum of a natural dolomite in Figure 9c, the two spectra are identical.

dissolution occurred on both substrates when fungi attacked planes of weakness (cleavage planes, grain boundaries and pore space) and fine-grained material that offered a large surface area. This yielded pitting, columnar structures and channels on the substrates (Figure 1c). Consequently, the porosity and permeability were enhanced.

[50] Alveolar-honeycomb structures found in soil and sediments are attributed to gas release (soil) or root encrustations associated with ectomycorrhizal fungi [Wright, 1986]. On rock surfaces, early studies attribute these morphologies to salt crystallization, whereby damage to the rock and eventual pitting or undercutting occurs when the pressure exerted by the preferential growth of large salt crystals exceeds the tensile strength of the rock [Rivas *et al.*, 2003; Parsons *et al.*, 2005].

[51] In the present study, these two structures (alveolar-honeycomb) were developed by the subaerial interaction of the fungi with the dolomitic substrates. The selective dissolution pattern by the fungal organic acids produced these two structures, which apparently have a different origin from that occurring in soil, sediment, or rock

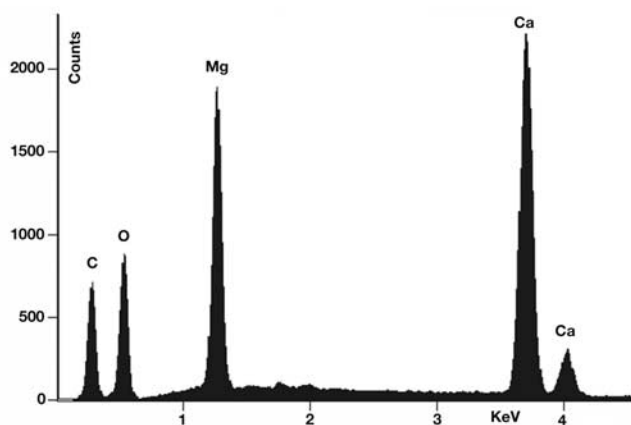


**Figure 9b.** Same as in 9a, but for the rhombic crystals in Figure 8b.

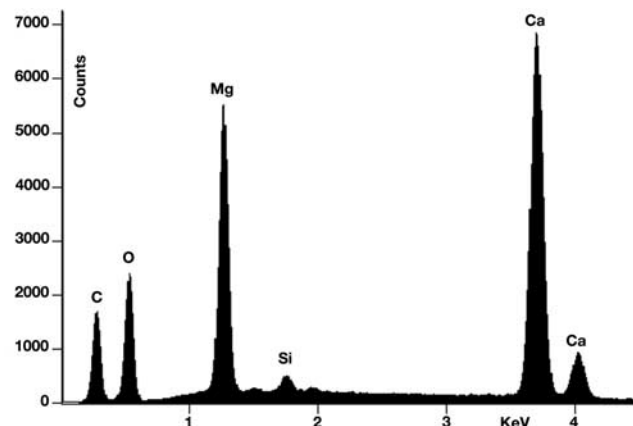


**Figure 9c.** EDX spectrum of natural dolomite crystals (see Figure 8c) from the experimental dolomitic substrates.

surfaces. Here the role of fungi could perhaps explain the origin of some alveolar-honeycomb weathering structures on rocks and buildings. Two aspects are characteristic of these structures: the boring of dolomite crystals that leaves chambers with standing walls, and the selective deposition of biominerals on the grain boundaries. It is highly significant that the fungi precipitated the biominerals on the grain boundaries only, leaving the chambers practically empty. The mineral external morphology was preserved (Figures 2a, 2b, 3a, and 3b). A paragenetic sequence of dissolution–deposition may be postulated here. As they are planes of weakness and are connected by matrices of finer grain size that are rich in organic matter, the grain boundaries have the following traits.

[52] 1. They offer easy conduits and an additional source of carbon for fungal proliferation and growth. The presence of organic and inorganic residues on a mineral surface within the mineral substrate is thought to encourage proliferation of fungi and other microbes [Burford *et al.*, 2003b]. The dolomites of Terwagne Formation are rich in organic matter along grain boundaries [Kolo *et al.*, 2002; Pr eat *et al.*, 2003], which offered the growing fungi an additional carbon source.

[53] 2. They favor mineral dissolution along grain boundaries and release  $\text{Ca}^{2+}$  and  $\text{Mg}^{2+}$  in the growth environment.

[54] 3. They provide preferential sites for Ca-oxalates precipitation. Since grain boundaries are regions of high energy they make excellent sites for the nucleation of precipitates.

[55] 4. They bring about dissolution (chemical boring) of matrix grains core. The selective boring of the middle parts of the grains may be interpreted as resulting from the temporary protection by the Ca-oxalates precipitate on the grain boundaries. The empty chambers also suggest that the deposition of the new biominerals preceded the dissolution (chemical boring) process. The continuation of the dissolution process led to the formation of true alveolar-honeycomb structures (Figures 3a, 3b, and 3c).

[56] In the present case, the fungi created microscopic networks within the rock matrix. As described above, although the fungi present were not burrowing Cryptocodoliths they were found to behave in the same way, as

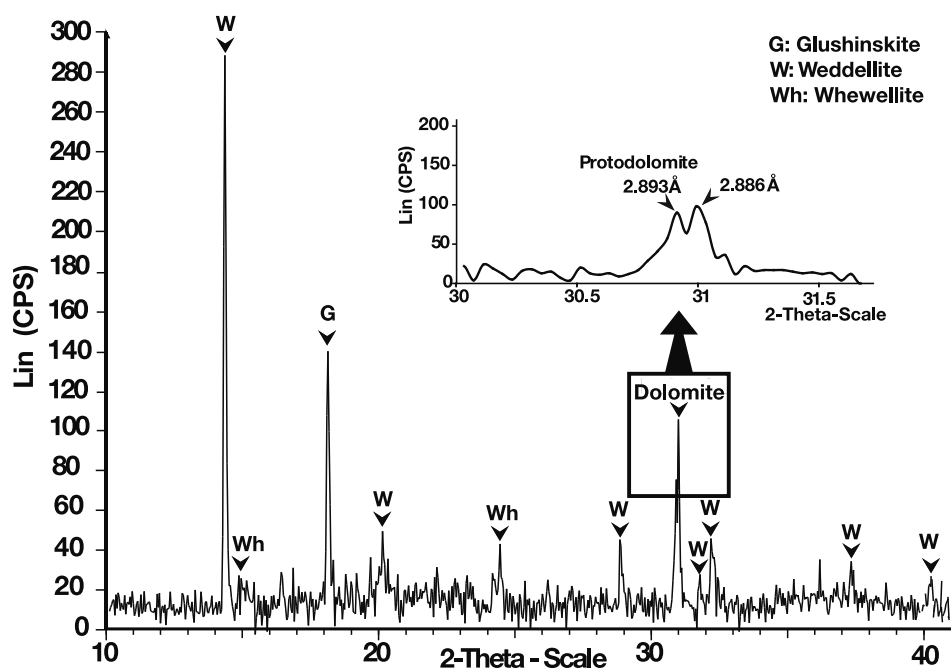


**Figure 9d.** The XRD spectrum of biominerals formed on the dolomitic substrates and embedded in the fungal mycelium and EPS layer. The spectrum shows the presence of Ca- and Mg oxalates (weddellite, whewellite, glushinskite) and a Ca-Mg biomineral as dolomite. The dolomite signal (inset figure) actually indicates two types: a protodolomite and a stoichiometric dolomite very much identical to the finding of *Rodriguez-Navarro et al.* [1997].

evidenced by the fact that the hyphal network appeared to be following a burrowed pore space (Figure 1d).

[57] The dolomite crystal in Figure 3c shows a selective diagonal dissolution-precipitation process in the direction of

the dissolution front. The diagonal dissolution is associated with simultaneous deposition of biominerals along the dissolved lines, suggesting an in situ dissolution-replacement process. The  $Mg^{2+}$  and  $Ca^{2+}$  released from

#### Typical XRD spectrum of Terwagne Formation dolomite

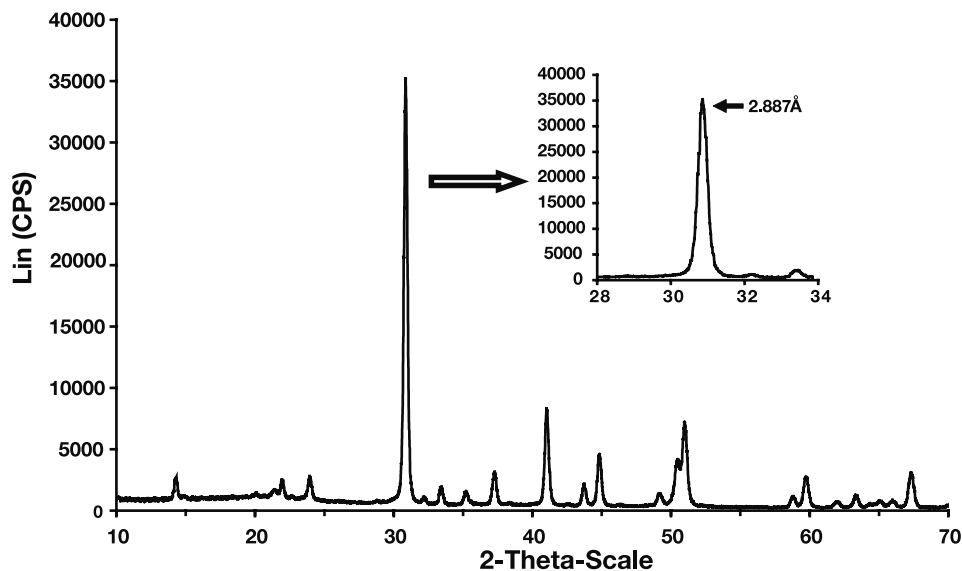


**Figure 9e.** The XRD spectrum of natural dolomite from dolomitic substrates of Terwagne Formation. The spectrum is quite different from the one in 9d, and the main dolomite peak (inset figure) does not show the characteristic double peak of dolomite recorded in Figure 9d suggesting an authigenic precipitation of dolomite in a fungal growth environment.

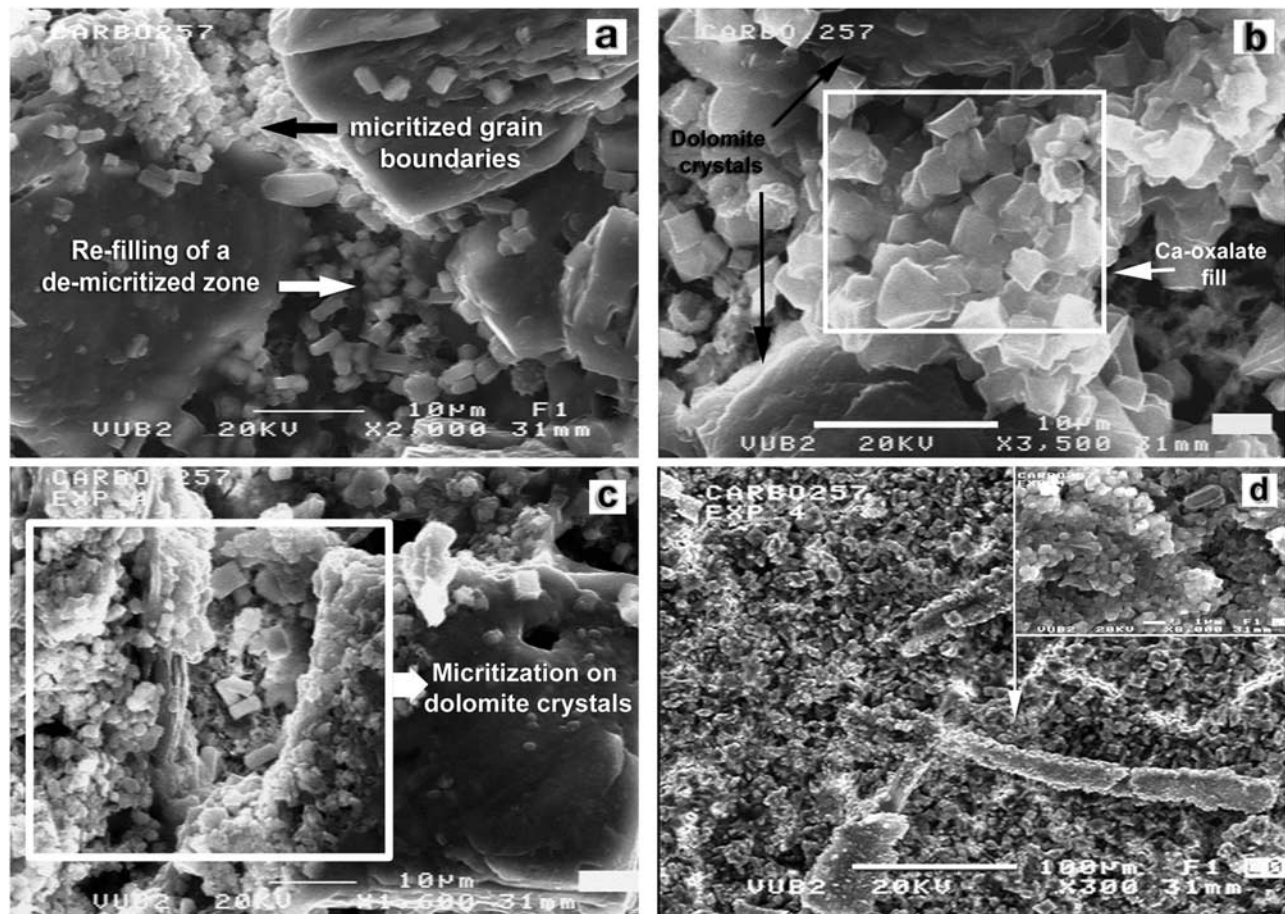


**Figure 10.** “Demicritization” and “micritization” of the carbonate substrates. (a) A dolomitic substrate demicritized by fungi. The fine-grained material (cement) filling in the space between the various grains has disappeared leaving the more resistant dolomitic crystals. Biominerals are replacing the old material that was consumed through fungal dissolution and chemical element uptake. The size of the new infill ranges between 2 and 3  $\mu\text{m}$ . (b) Fungal micritization of the demicritized space between original dolomite crystals. The micritization process involved the precipitation of biominerals of much smaller grain size ( $\sim 1 \mu\text{m}$ ) in the porous space between grains. It is also a process of cement formation and grain bridging. (c) Grain micritization. The fungally produced biominerals are precipitated directly on the original dolomite crystals in a process of dissolution and precipitation. Eventually this process will result in cementation or in total replacement. (d) Total substrate micritization. The micron-size biominerals formed new substrates that either replaced or superposed the old ones. Notice also the highly biomineralized fungal hyphae littering the surface. All are SEM photomicrographs, dolomitic thin sections, Terwagne Fm., France; bar scale = 10  $\mu\text{m}$ .

the dolomite crystal substrate through the dissolution process reacted with fungal metabolites (organic acids) and precipitated oxalates across the dissolution front. The newly formed minerals are aligned in straight lines along the dissolution front. As was shown in Figure 12, this process could lead to total replacement by biominerals.

#### 4.3. Biomechanical Role of Fungal Hyphae

[58] Biochemical diagenesis preceded the biomechanical one. In Figure 1d, the fungal hyphae formed a network that horizontally penetrated the dolomitic substrate. Although the present fungi are not real burrowing cryptoendoliths, their network within the attacked substrate showed a similar ability. The hyphal network did not seem to follow an

original pore space but rather a burrowed one (Figure 1d). The hyphal network is generally at a lower level than the substrate surface and the hyphae circumvented the dolomite grains by passing through the space between grain boundaries. The availability of this space indicates a predissolution process of fine-grained material (micrite) followed by fungal hyphae penetration, a suggestion that is in accordance with the absence of fine-grained material in several parts of the substrate (Figure 1d).

[59] Fungal hyphae growth produces mechanical pressure that may dislodge matrix grains and cause substrate disintegration [Chen *et al.*, 2000; Sterflinger, 2000; Warscheid and Braams, 2000; Burford *et al.*, 2003b; Hoffland *et al.*, 2004], thus increasing the surface area exposed to fungal

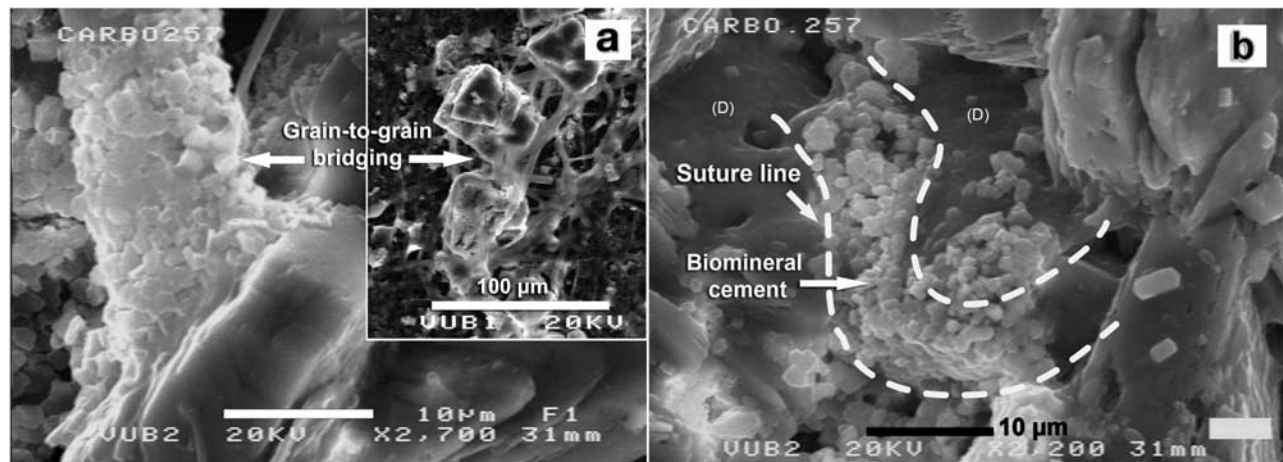


**Figure 11.** Grain-grain bridging and bio-cementation by fungi. (a) Dolomitic substrate showing a process of grain-grain bridging. The two dolomite crystals are connected by a bridge of biominerals precipitated by fungal interaction with the substrate. Fungal hyphae and EPS material occupying the intergranular space can form a base for biominerals deposition and thus enhance grain-grain bridging. (b) Typical grain-grain cementation process. The micron-size ( $\sim 1 \mu\text{m}$ ) biomineral cement “welds” the two grains together and leaves suture lines along the cemented area. All are SEM photomicrographs, dolomitic thin section, Terwagne Fm., France; bar scale =  $10 \mu\text{m}$  respectively.

organic acids. This enhances the biochemical dissolution of the substrate minerals.

#### 4.4. Formation of Biominerals

[60] The formation of the different types of biominerals by fungal interaction is generally controlled by metal type and availability in the mineral substrate, although this is not always the case [Lee and Parsons, 1999; Arocena et al., 2003]. The calcitic substrate produced only Ca-bearing biominerals (weddellite and whewellite). The dolomitic substrates produced Mg, Ca (glushinskite, weddellite, and whewellite), P (possibly struvite) and Mg-Ca bearing biominerals. All the Mg and P bearing biominerals were solely formed on the dolomitic substrate. The EDX, XRD and Raman analyses confirmed the composition of these biominerals (Figures 4, 5, 6, 7, and 9d). The Mg and Ca metals were both mobilized from the dolomite substrate while the growth medium provided phosphorus. The insertion of substrate metals into the new biominerals suggests an important cycling and redistribution of metals where fungi are the major players, contributing thus to the formation of new sediments and soils.

##### 4.4.1. Mg-Ca Biomineral

[61] The fourth biomineral group from the dolomite substrate, composed of Mg-Ca, was identified by EDX and XRD. The biominerals have rhombic crystal forms (Figures 8a and 8b) that are similar to dolomite crystals (Figure 8c) and occur within the fungal mycelium, clearly above the thin section substrate, thus suggesting that they are newly precipitated crystals. The crystals (Figure 8a) show no signs of fungal attack (dissolution, boring or biomineral surface precipitation). These crystals were originally embedded in the fungal mass on the substrate-EPS layer interface. The SEM-EDX analysis of these crystals gave a composition of Ca, Mg, C and O (Figure 9a and 9b). This spectrum is identical to the EDX spectrum of dolomite crystals of the Terwagne Formation (Figure 9c).

The XRD analysis of the fungal mass alone shows a mineral composition of weddellite, whewellite, glushinskite and a dolomite signal (Figure 9d). Rodriguez-Navarro et al. [1997] reported the formation of authigenic dolomite within alteration crusts developing on the limestone surface of a historical building, where two different types of authigenic dolomite occurred: limpid stoichiometric dolomite and Ca-rich ‘protodolomite’. The main mechanism in the formation of this type of dolomite as proposed by these authors involved a high concentration

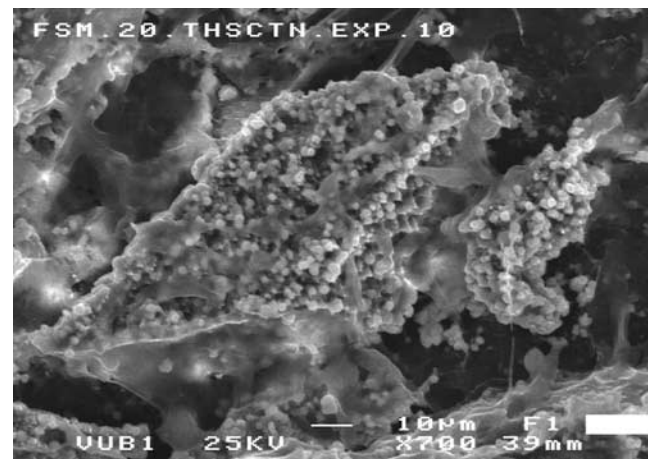


**Figure 12.** SEM photomicrograph of total replacement induced by fungal interaction with limestone substrate. The calcite crystal is totally replaced by biominerals produced during the interaction, while the original rhombic shape is preserved intact. The lines are straight and sharp, indicating a simultaneous dissolution and replacement. Image is a limestone thin section, Morrone di Pacentro Fm. Italy; bar scale =  $10 \mu\text{m}$ .

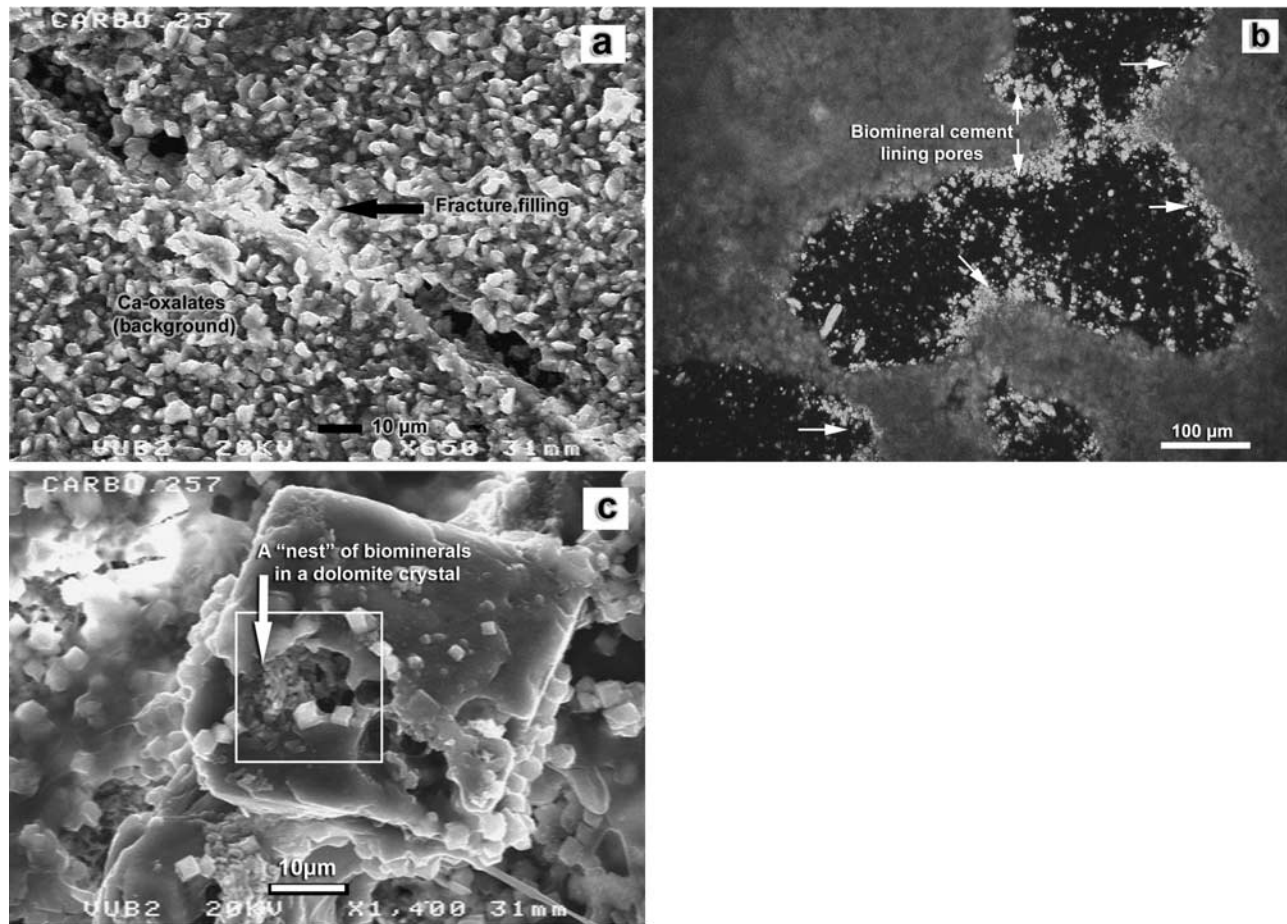


**Figure 13.** Cavity filling and formation of microporosity. (a) A natural fracture on dolomitic substrate being filled with the newly formed biominerals (oxalates). The middle part of the fracture is nearly filled, and it shows the same texture as the rest of substrate surface, where extensive deposition of biominerals has occurred. (b) A large view of original porosity being filled with biominerals as fringing cement lining the inner contour of the pore as well as partially littering the pore. Optical microscope was used, XPL, Morrone di Pacentro Fm. Italy; bar scale = 100  $\mu\text{m}$ . (c) A dolomite crystal showing fungally produced intragranular porosity being refilled with biominerals. The fill is composed of micron-size crystals “laid” in the “nest”. The size of the biomineral crystals outside the nest is larger, suggesting a different process or controls of formation. Figures 13a and 13b are SEM photomicrographs, dolomitic thin sections, Terwagne Fm., France; bar scale = 10  $\mu\text{m}$ .

of Mg, achieved by selective Ca removal, formation of microenvironment, presence of  $\text{CO}_3^{2-}$ ,  $\text{CO}_3\text{H}^-$ , and  $\text{CO}_2$ , and microbial activity (fungi and bacteria).

[62] The pattern of XRD spectrum of the dolomite identified in this study is very much identical to the one published by *Rodríguez-Navarro et al.* [1997, Figure 3] for an authigenic and microbially precipitated dolomite. The double peak dolomite spectrum at  $d$  spacing = 2.893Å represents a high Ca-dolomite (protodolomite), and at  $d$  spacing = 2.886Å a stoichiometric dolomite (Figure 9d, inset). The XRD spectrum (Figure 9e) of the original dolomite from the same rock sample as the thin section substrate (sample 40 Terwagne Formation) is totally different and is characterized by the single high peak at  $d$  spacing = 2.887Å, which is in the range of stoichiometric dolomites [*Jones et al.*, 2001]. The formation of dolomite

under these conditions suggests the possibility of recycling of existing dolomite by microbial interaction.

#### 4.4.2. Sequence of Biomineralization

[63] In this study, the Mg- and the Mg-Ca biominerals generally superposed Ca-oxalates in thin sections, indicating a post-Ca-oxalates formation. This sequence of biomineralization may indicate the availability and relative importance of Ca and Mg cations in the fungal growth environment. In the case of a dolomitic substrate, it may also illustrate the sequence of possible uptake-expulsion processes for  $\text{Ca}^{2+}$  and  $\text{Mg}^{2+}$  by fungi. Fungi first neutralize the toxicity of excess  $\text{Ca}^{2+}$  through  $\text{Ca}^{2+}$  uptake and subsequent precipitation of Ca-oxalates [*Gadd*, 1999; *Sterflinger*, 2000]. The resulting solutions are rich in Mg within the fungal growth environment and can precipitate glushinskite and Ca-Mg biominerals. The restricted spatial distribution of these Mg- biominerals on the thin sections

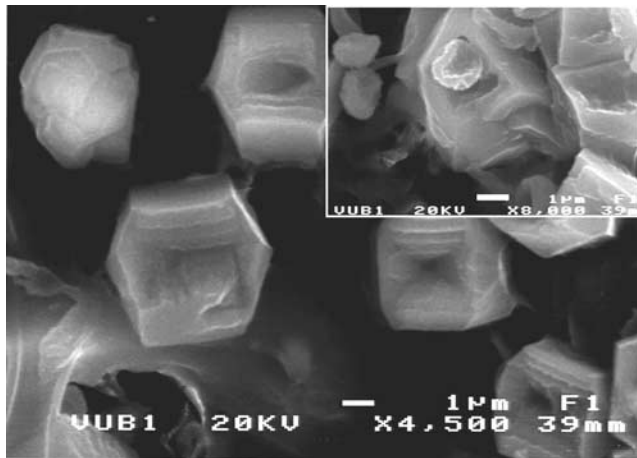


**Figure 14.** SEM photomicrograph showing a possible ooidal structure predecessor formed through fungal interaction with carbonate substrate. These crystal structures are concentric and show zonation. The inset figure shows that a fungal spore originally occupied the oval center, hence the nucleation site. Images are from Morrone di Pacentro Fm. Italy; bar scale = 1  $\mu\text{m}$ .

as well as within the fungal mass suggests that the high Mg concentration necessary for its precipitation only prevailed in localized microenvironments. In these microenvironments, high Mg/Ca ratio is achieved by accentuated leaching and continuous removal of Ca as oxalates. However, besides the “protodolomite” of *Rodríguez-Navarro et al.* [1997] a hydrous form of Ca-Mg carbonate has been postulated by some authors as a precursor dolomite [*Kelleher and Redfern, 2002*]. The formation of Ca-Mg biominerals through fungal interaction with the original dolomitic substrate is confirmed in this study, although further investigation concerning their dolomitic nature and formation mechanism is needed.

#### 4.5. Petrography of the New Substrate

[64] The “demictization” process, in its early stages, leaves only the larger crystals of dolomite or calcite on the substrates and increases porosity and permeability (Figure 10a). This process affected the calcitic substrates more than the dolomitic ones, owing to the higher solubility of calcite compared to dolomite, which could lead to the total dissolution of the substrate. The “micritization” process as a whole induced the formation of new micron sized material either as new cement that fills pore space (inter-

granular and intragranular) in the original substrate or as sheets or layers precipitated on or even replacing the original surfaces (Figures 10a–10c, 12, and 13a–13c). The new “micrite” is precipitated, owing to inputs by recycled autochthonous elements (mainly  $\text{Ca}^{2+}$  and  $\text{Mg}^{2+}$ ) from the original substrate. It is interesting to note that biominerals precipitating directly in between grains are always of much smaller size ( $\pm 1 \mu\text{m}$ ). This could be related to the space available for crystal growth [*Kavanagh, 1995*] and to a simultaneous fast dissolution and precipitation process. In the present study, the action of the fungi on the substrate grains is similar to endolithic, epilithic and chasmolithic microorganisms acting upon grains in natural environments [*Schneider and Le Campion, 1999; Hillgartner et al., 2001; Garcia-Valles et al., 2002*].

##### 4.5.1. Role of the New “Biomineral Cement”

[65] The grain-to-grain bridging and cementation processes both follow the “demictization” and the “micritization” of the substrate matrix and of the dolomite and calcite crystals. Bridging of the grains on both substrates, dolomitic and calcitic, took place via biomineral bridges and biomineralized fungal hyphae. An example of a pure biomineral bridge can be seen in Figures 10a–10c. The original cementing material between the two dolomite crystals was removed by fungi and replaced by the newly micrite-size biominerals. This biomineral bridge is analogous to the micritic meniscus-type cement formed by microbially induced precipitation of micrite in carbonate sands [*Hillgartner et al., 2001*].

[66] Biominerals form dense encrustations on fungal hyphae endogenously and exogenously [*Arnott, 1995; Kolo and Claeys, 2005*]. The size of the encrusting biominerals usually does not exceed 1  $\mu\text{m}$  (Figures 10d and 11a). Figure 11a shows one typical case of grain-to-grain bridging by fungal hyphae. The base of the biomineralized hyphae appears to be well attached to the surface of the dolomite crystal making a “natural” mineral extension from the surface. The inset (Figure 11a) shows an overview of fungal hyphae as a biomineral bridge, and also a biomineral bridge deposited between two grains. In nature, calcified cyanobacterial filaments played the same role as bridges and were involved in micrite formation and cementation, which *Perry* [1999] called “constructive micrite envelopes”. This view likely applies to the role of fungi interacting with carbonate substrates. A destructive phase characterized by dissolution, demictization and substrate disintegration is followed by a constructive phase where micritization, recementation, and neo-substrate formation take place.

**Table 2.** The  $\delta^{13}\text{C}$  and  $\delta^{18}\text{O}$  of Water Used in Fungal Growth

Samples	Isotopic Values of Water Samples		
	$\delta^{13}\text{C}$	$\delta^{18}\text{O}$	$\delta^{18}\text{O}$ smow = $-7.1$ per mille Corrected Values
MilliQ water	-28.709	-7.656	-7.050
	-28.760	-7.749	-7.150
	-28.703	-7.747	-7.150
Deionized water	-28.727	-7.634	-7.034
	-28.709	-7.624	-7.020

[67] Cementation (more precisely recementation) in these carbonate substrates is chemically controlled by the fungally induced dissolution. The cementing material (newly formed biominerals) is produced by the reaction of fungal organic acids with calcium and magnesium released from the substrate itself. This material, besides bridging the substrate grains, forms new cement that replaces the original one. In the present study cementing developed so well that it was possible to trace suture lines between two dolomite crystals (Figure 11b). Microbially induced cementation of carbonate rocks and the micritic meniscus cements could be considered a signature of vadose cementation [Hillgartner *et al.*, 2001]. In the present study the deposition of very fine crystal material on the original substrate grains induced by fungal action appears to be similar in results to microbially induced vadose zone cementation.

[68] Carbonate grains may be bored by fungi, bacteria and algae. Fine-grained (micrite) carbonate (aragonite, high-Mg calcite) may then precipitate in holes. In some cases, only the exteriors of grains are affected – micrite rims/envelopes. In other cases, grains may be completely micritized. The present cement shares common features with the sedimentary calcium carbonate cement, i.e., precipitated chemically during diagenesis, replacing old material, having a clear and clean appearance, showing sharp contacts between cement and grains, and deposition in primary and secondary pore space. Although the various types of cements in carbonate sediments are well defined in the literature, the present study proposes a new type of diagenetic cement in carbonate rock that is not related to the common diagenesis cements. This new cement is neither carbonate nor siliceous. It is referred to here as “biomineral cement”.

#### 4.5.2. Biomineral Metasomes and Metacrysts

[69] Typical crystal replacement occurred by the new biominerals. Figure 12 shows a calcite crystal from a calcitic substrate totally replaced by new biominerals. The original form and lines have been well preserved suggesting that the process involved two simultaneous chemical reactions, one, dissolution of the paleosome (calcite crystal) and the other, precipitation of the metasome (biominerals) that proceeded (supposedly) at the same volumetric rate that formed the new biomineral metacrysts. Evidence of dissolution-simultaneous precipitation has already been presented (Figure 3c). Other cases of evidence of diagenetic mineral replacement by fungal interaction are the alveolar-honeycomb structures (Figures 2 and 3), where the structures are clearly formed by a dissolution that volumetrically exceeded the precipitation of the secondary biominerals, and then simply created a mouldic pore that could be reduced by some type of cement, much like some of the above biominerals. In both of these cases ghost images of the original crystal/fabric are formed.

#### 4.5.3. Zonal Structures

[70] The polygonal concentric zonation in some biomineral crystals (Figure 14) is a reflection of changes in the growth microenvironment (mainly pH and cation availability) during crystal growth. The structures are evidently not closed yet; otherwise the concentric structure would not be visible. Zonal nucleation has happened around the fungal spores, and is widely spread in the growth environment. Figure 14 (inset) shows a fungal spore still occupying the oval nucleation site. It is plausible to suggest the

existence of these concentric structures in completely closed forms; their abundance might also be higher than observed. Such concentric structures, although visibly different in size and mechanism of formation, are perhaps reminiscent of those observed in sedimentary ooids. Thus far, it has not been possible to speculate further on the position of these zoned particles in carbonate diagenesis, but it is worth mentioning that fungal ooids have been reported previously [Krumbein *et al.*, 2003].

#### 4.6. New Isotopic Signature

[71] The stable isotopes of new minerals produced by fungi-rock interaction could indicate substrate diagenesis. Garvie *et al.* [2000] found that a biomineralized micritic layer formed by the fungal mycobiont of endolithic lichen is enriched in  $^{13}\text{C}$ , relative to the underlying caliche, indicating that the light carbon is taken up into organic material, hence leaving heavier  $\text{CO}_2$  to form carbonate. The heavy  $^{13}\text{C}$  enrichment suggested a biologically induced fractionation rather than biological precipitation. In the present case, compared to aforementioned natural micritic layer, the newly formed minerals and the attacked surfaces show a considerable depletion in  $^{13}\text{C}$ . This depletion suggests a direct biological involvement in the isotopic fractionation and mineral formation. The differences in isotopic compositions reflect the strong effect of organically incorporated  $^{13}\text{C}$ . The source of the carbon and oxygen in the newly formed minerals is unclear. Possible sources include the substrate (dissolution of  $\text{CO}_3^{2-}$ ), the atmosphere ( $\text{CO}_2$  in solution), and the water used in the experiment. In ancient strata, especially in calcretes and paleosols, these differences in  $^{13}\text{C}$  could indicate previous microbial action.

#### 4.7. Substrate Formation, Biostratification, and Accretion Versus “Biological Weathering”

[72] The fungi that spread over and covered the experimental substrates with the EPS layer developed a consistent and dense layer of biominerals over the original substrates. These new layers, which are generally fine-grained (1–5  $\mu\text{m}$ ) but may also be of larger size (5–10  $\mu\text{m}$ ), are superposed on the original substrates. Their superposition produces micrometer-scale “biostratification” that is comparable to accretion layering in cyanobacterial stromatolites. The Ca-oxalates forming the majority of the newly formed minerals are composed of weddellite and, to a lesser extent, whewellite.

[73] Glushinskite, the Mg-oxalate, is deposited on the Ca-oxalates layer on the dolomitic substrates (Figure 15). Consequently, in agreement with the general rule of superposition, the deposition of the Mg-oxalates must occur after that of the Ca-oxalate. This is related to Mg and Ca solubility. Mg deposition as oxalates occurs after the lowering of Ca concentration in the growth environment as a detoxification process by fungi [Kolo and Claeys, 2005].

[74] Fungal dissolution of carbonate substrates is a clear form of biological weathering. Some of the experimental substrates were completely dissolved by the fungi, and replaced by new biomineralized substrates. In the experiment, a 30  $\mu\text{m}$  carbonate substrate (thin section thickness) was removed in only 15 days. Although this result was produced under laboratory conditions, it still reflects the strong weathering that fungi may induce on exposed car-

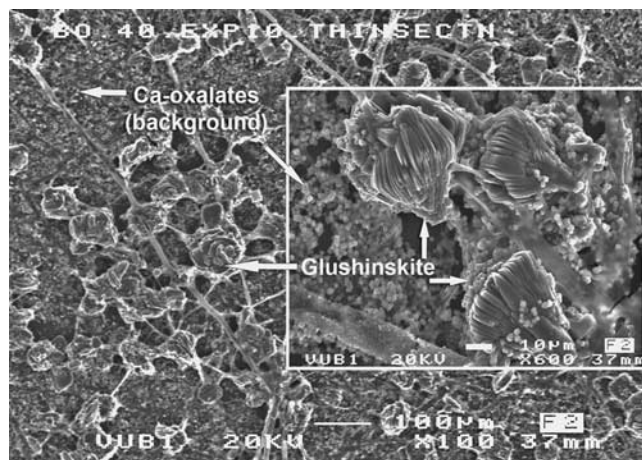


**Figure 15.** SEM photomicrograph showing glushinskite, the Mg-oxalate deposited on the Ca-oxalates layer on the dolomitic substrates. This superposition suggests that the deposition of the Mg-oxalates occurred after the Ca-oxalate deposition, creating thus, “biological stratification”. The inset figure shows the clear superposition and the extent and size of Ca-oxalates that form the background. Image is a dolomitic thin section, Terwagne Fm., France; bar scale = 100  $\mu\text{m}$ .

bonate substrates. The question here is whether accretion exceeds, is less or equal to biological weathering. Under natural field conditions, there is generally a fungally produced “micritic layer” underlying the fungal mass on rock surfaces [Wilson *et al.*, 1980; Garvie *et al.*, 2000; Duane *et al.*, 2003; Etienne and Dupont, 2002; Arocena *et al.*, 2003]. Moreover, since a thick rock stratum underlies the micritic layer it would be difficult to assume that the fungal weathering is the predominant process. Biostratification is produced in both experimental and natural cases.

## 5. Conclusions

[75] The role of fungi may be of great significance in the diagenesis of carbonate rocks. In the present study, the fungal interaction with carbonate substrates (thin sections and rock chips) triggered specific diagenetic processes that produced significant diagenesis of substrates’ petrography and chemistry, in many aspects comparable to sedimentary diagenesis. The diagenetic processes included substrate dissolution, neo-mineral formation, biomineralization, micritization, demicritization, grain-to-grain bridging, cementation, replacement, open-space filling, porosity permeability enhancement grain size alteration, concentric zonation structures, isotopic fractionation, neo-substrate formation and biostratification. These processes, driven by the biochemical (organic acids) and biomechanical (growth pressure) potency of fungi, introduced new textures and structures, i.e., alveolar-honeycomb, mouldic-replacement porosity, intergranular and intragranular porosity, whole crystal replacement, and zonal-concentric structures. Original carbonate cement was removed through a demicritization process. A new type of micrite-size cement, named here “biomineral cement”, was formed between the grains

in the form of bridging-meniscus cement and as biomineralized fungal hyphae. This new cement also lined pores in similar mode to spar cement. Dolomite or calcite crystals from the substrates were micritized by dissolution-biomineral precipitation on their surfaces. Fungal interaction produced “biological stratification” when new substrates, totally composed of micrite-size biominerals (mainly Ca- Mg- oxalates), were precipitated on the original calcitic or dolomitic substrates.

[76] Fungal interaction significantly altered the isotopic and mineralogical composition of the substrates. The isotopic signature of the newly formed biominerals is considerably different from the signature of the substrates, suggesting a significant isotope fractionation. Compared to the original unattacked surfaces, the  $\delta^{13}\text{C}$  of the newly formed minerals and attacked substrates show considerable depletion while the  $\delta^{18}\text{O}$  values show enrichment.

[77] Mineralogically, Ca and Mg were recycled from calcite and dolomite into the newly formed biominerals: weddellite, whewellite, glushinskite, protodolomite and possibly struvite, where they filled voids, selectively precipitated on grain boundaries, biomineralized fungal hyphae, and also formed new substrates. This recycling was selective and reflected the chemistry of the substrate. Mg-biominerals (oxalates, protodolomite and possible struvite) were only formed on dolomitic substrates, while Ca-biominerals were formed on both calcitic and dolomitic ones. Of particular significance was the formation of ‘protodolomite’ during fungal interaction with the dolomitic substrate. The formation of this “protodolomite” may signal an unprecedented case of a sedimentary dolomite being recycled within a fungal-carbonate substrate environment.

[78] In the present study, the role of fungi in the diagenesis of carbonate rocks significantly exceeded that of simple surface bioweathering, the results approaching those of sedimentary diagenesis, where petrography, mineralogy and chemistry are changed. This role shows fungi to be important players in the redistribution of metals, especially Ca, Mg and C and reshaping rock surfaces.

[79] **Acknowledgments.** We thank J. Vereecken, O. Steenhaut and K. Baerts, Department of Metallurgy, Vrije Universiteit Brussels, for the SEM-EDX and Raman facilities, and for valuable technical assistance. We also thank A. Bernard, Department of Geology, Université Libre de Bruxelles for the XRD facility. Special thanks go to Anna Gorbushina, ICBM-Oldenburg University, Germany, for valuable comments. This work is supported by the Onderzoekraad van de Vrije Universiteit Brussel.

## References

- Arnott, H. J. (1995), Calcium oxalates in fungi, in *Calcium Oxalates in Biological Systems*, edited by S. R. Khan, pp. 73–111, CRC Press, Boca Raton, Fla.
- Arocena, J. M., L. P. Zhu, and K. Hall (2003), Mineral accumulations induced by biological activity on granitic rocks in Qindhai Plateau, China, *Earth Surf. Processes Landforms*, 28, 1429–1437.
- Bentis, C. J., L. Kaufman, and S. Golubic (2000), Endolithic fungi in reef-building corals (Order: Scleractinia) are common, cosmopolitan, and potentially pathogenic, *Biol. Bull.*, 198, 254–260.
- Bruni, R. (2003), Stratigraphie du Crétacé inférieur de la Maiella (Abruzzes) et des Préalpes (Frioul), Italie, Ph.D. thesis, 237 pp., Univ. Libre Bruxelles, Brussels.
- Burford, E. P., M. Kierans, and G. M. Gadd (2003a), Geomycology: Fungi in mineral substrata, *Mycologist*, 17, 98–107.
- Burford, E. P., M. Fomina, and G. M. Gadd (2003b), Fungal involvement in bioweathering and biotransformation of rocks and minerals, *Miner. Mag.*, 67, 1127–1155.

- Caplan, T. B. (1994), Reporting of stable hydrogen, carbon and oxygen isotopic abundances, *Pure Appl. Chem.*, *66*, 1837–1849.
- Chen, J., H. P. Blume, and L. Beyer (2000), Weathering of rocks induced by lichen colonization—A review, *Catena*, *39*, 121–146.
- Craig, H. (1957), Isotopic standards for carbon and oxygen and correction factors for mass-spectrometric analysis of carbon dioxide, *Geochim. Cosmochim. Acta*, *12*, 133–149.
- Duane, J., A. Al-Mishwat, and M. Rafique (2003), Weathering and karst development on marine terraces, northwest Morocco, *Earth Surf. Processes Landforms*, *28*, 1439–1449.
- Etienne, S., and J. Dupont (2002), Fungal weathering of basaltic rocks in cold oceanic environment (Iceland: Comparison between experimental and field observations), *Earth Surf. Processes Landforms*, *27*, 737–748.
- Frost, L. R., and L. M. Weier (2003a), Thermal treatment of weddellite—A Raman and infrared emission spectroscopic study, *Thermochem. Acta*, *406*, 221–232.
- Frost, L. R., and L. M. Weier (2003b), Raman spectroscopy of natural oxalates at 298 and 77K, *J. Raman Spectrosc.*, *34*, 776–785.
- Frost, L. R., and L. M. Weier (2004), Thermal treatment of whewellite—A thermal analysis and Raman spectroscopic study, *Thermochem. Acta*, *409*, 79–85.
- Frost, L. R., M. Adebajo, and L. M. Weier (2004), A Raman spectroscopic study of thermally treated glushinskite—The natural magnesium oxalate dehydrate, *Spectrochim. Acta, Part A*, *60*, 643–651.
- Gadd, G. M. (1999), Fungal production of citric and oxalic acid: Importance in metal speciation, physiology and biogeochemical processes, *Adv. Microb. Physiol.*, *41*, 47–92.
- Gadd, G. M. (2002), Fungal influence on mineral dissolution and metal mobility: Mechanisms and biogeochemical relevance, paper presented at 12th Annual Goldschmidt Conference, Eur. Assoc. of Geochem., Davos, Switzerland.
- Gadd, G. M., E. P. Burford, M. Fomina, F. A. Harper, and H. Jacobs (2002), Fungal influence on metal mobility: Mechanisms and relevance to environment and biotechnology, paper presented at 7th International Mycology Congress, Oslo Univ., Oslo, August.
- García-Valles, M., C. Urzi, and M. Vendrell-Saz (2002), Weathering processes on the rock surface in natural outcrops: The case of an ancient marble quarry (Belevi, Turkey), *Environ. Geol.*, *41*(8), 889–897.
- Garvie, L. A. J., F. Bungartz, T. H. Nash, and L. P. Knauth (2000), Caliche dissolution and calcite biomineralization by the endolithic lichen *Verucaria rubrocincta* Breuss in the Sonoran desert, paper presented at 10th Annual Goldschmidt Conference, Eur. Assoc. for Geochem., Oxford, U. K.
- Gharieb, M. M., J. A. Sayer, and G. M. Gadd (1998), Solubilization of natural gypsum (CaSO<sub>4</sub>·2H<sub>2</sub>O) and the formation of calcium oxalate by *Aspergillus niger* and *Serpula himantioides*, *Mycol. Res.*, *102*, 825–830.
- Golubic, S., G. Brent, and T. Le Campion (1970), Scanning electron microscopy of endolithic algae and fungi using a multipurpose casting-embedding technique, *Lethaia*, *3*, 203–209.
- Golubic, S., R. Gudrun, and T. Le Campion-Alsumard (2005), Endolithic fungi in marine ecosystems, *Trends Microbiol.*, *13*(5), 229–235.
- Hendricks, J. J., R. J. Mitchell, K. A. Kuehn, S. D. Pecot, and S. E. Sims (2006), Measuring external mycelia production of ectomycorrhizal fungi in the field: The soil matrix matters, *New Phytol.*, *171*, 179–186.
- Hillgartner, H., C. Duparez, and W. Hug (2001), Microbially induced cementation of carbonate sands: Are micritic meniscus cements good indicators of vadose diagenesis?, *Sedimentology*, *48*, 117–131.
- Hoffland, E., R. Giesler, T. Jongmans, and N. van Breemen (2002), Increasing feldspar tunneling by fungi across a North Sweden podzol chronosequence, *Ecosystems*, *5*, 11–22.
- Hoffland, E., et al. (2004), The role of fungi in weathering, *Front. Ecol. Environ.*, *2*(5), 258–264.
- Jackson, R. B., J. Canadell, J. R. Ehleringer, H. A. Mooney, O. E. Sala, and E. D. Schulze (1996), A global analysis of root distribution for terrestrial biomass, *Oecologia*, *108*, 389–411.
- Jones, B., L. W. Robert, and A. J. MacNeil (2001), Powder X-ray diffraction analysis of homogeneous and heterogeneous sedimentary dolostones, *J. Sed. Res.*, *71*, 790–799.
- Jones, E. B. G. (1994), Fungal adhesion, *Mycol. Res.*, *98*, 961–981.
- Kavanagh, J. P. (1995), Calcium oxalate crystallization in vitro, in *Calcium Oxalates in Biological Systems*, edited by S. R. Khan, pp. 1–21, CRC Press, Boca Raton, Fla.
- Kelleher, J. I., and A. T. Redfern (2002), Hydrous calcium magnesium carbonate, a possible precursor to the formation of sedimentary dolomite, *Mol. Simul.*, *28*(6–7), 557–572.
- Kolo, K., and P. Claeys (2005), In vitro formation of Ca-oxalates and the mineral glushinskite by fungal interaction with carbonate substrates and seawater, *Biogeochemistry*, *2*, 451–497.
- Kolo, K., B. Mamet, and A. Pr at (2002), Dichotomous filamentous dolomite crystal growth in the Lower Carboniferous from northern France: A possible direct production of fungal activity?, in *Proceedings of the First Geologica Belgica International Meeting*, edited by P. Degryse and M. Sintubin, pp. 117–120, Aardk. Mededel., Leuven, Belgium.
- Krumbein, E. W., U. Brehm, G. Gerders, A. Gorbushina, G. Levitt, and K. Palinska (2003), Biofilm, biocitron, biomat, microbiolites, oolites, stromatolites geophysiology, global mechanism, parahistology, in *Fossil and Recent Biofilms*, edited by W. E. Krumbein et al., pp. 1–27, Springer, New York.
- Landeweert, R., E. Hoffland, R. D. Finlay, T. W. Kuyper, and N. van Breemen (2001), Linking plants to rocks: Ectomycorrhizal fungi mobilize nutrients from minerals, *Trends Ecol. Evol.*, *16*(5), 248–254.
- Landeweert, R., C. Veenman, T. W. Kuyper, H. Fritze, K. Wernars, and E. Smit (2003), Quantification of ectomycorrhizal mycelium in soil by real-time PCR compared to conventional quantification techniques, *FEMS Microbiol. Ecol.*, *45*, 283–292.
- Lee, M. R., and I. Parsons (1999), Biomechanical and biochemical weathering of lichen-encrusted granite: Textural controls on organic-mineral interactions and deposition of silica-rich layers, *Chem. Geol.*, *161*, 385–397.
- Mamet, B., and A. Pr at (2005), S dimentologie du Vis en d’Avesnes-sur-Helpe (Avenois, nord de la France), *Geol. Belgica*, *8*, 17–26.
- McCrea, J. M. (1950), On the isotopic chemistry of carbonates and a paleotemperature scale, *J. Chem. Phys.*, *18*, 849–857.
- Parsons, R. L., J. W. Head III, and D. R. Marchant (2005), Weathering pits in the Antarctic dry valleys: Insolation-induced heating and melting, and applications to Mars, *Lunar Planet. Sci.*, *XXXVI*, 1138.
- Perry, C. (1999), Biofilm-related calcification, sediment trapping and constructive micrite envelopes: A criterion for the recognition of ancient grass-bed environments?, *Sedimentology*, *46*, 33–45.
- Pr at, A., K. Kolo, B. Mamet, A. Gorbushina, and D. Gillan (2003), Fossil and subrecent fungal communities in three calccrete series from the Devonian of the Canadian Rocky Mountains, Carboniferous of northern France and Cretaceous of central Italy, in *Fossil and Recent Biofilms*, edited by W. E. Krumbein et al., pp. 307–323, Springer, New York.
- Rios, A., and C. Ascaso (2005), Contributions of in situ microscopy to the current understanding of stone bioteriation, *Int. Microbiol.*, *8*, 181–188.
- Rivas, T., B. Prieto, B. Silva, and J. M. Birginie (2003), Weathering of granitic rocks by chlorides: Effect of the nature of the solution on weathering morphology, *Earth Surf. Processes Landforms*, *28*, 425–436.
- Rodr guez-Navarro, C., E. Sebasti n, and M. Rodr guez-Gallego (1997), An urban model for dolomite precipitation: Authigenic dolomite on weathered building stones, *Sed. Geol.*, *109*, 1–11.
- Rosling, A., B. D. Lindhal, A. F. S. Taylor, and R. D. Finlay (2004), Mycelial growth and substrate acidification of ectomycorrhizal fungi in response to different minerals, *FEMS Microbiol. Ecol.*, *47*, 31–37.
- Russ, J., R. L. Palma, D. H. Loyd, T. W. Boutton, and M. Coy (1996), Origin of the whewellite-rich rock crust in the lower region of southwest Texas and its significance to paleoclimatic reconstructions, *Quat. Res.*, *46*, 27–36.
- Sayer, J. A., and G. M. Gadd (1997), Solubilization and transformation of insoluble inorganic metal compounds to insoluble metal oxalates by *Aspergillus niger*, *Mycol. Res.*, *101*, 653–661.
- Schneider, J., and T. Le Campion (1999), Construction and destruction of carbonates by marine and freshwater cyanobacteria, *J. Phycol.*, *34*, 417–426.
- Sterflinger, K. (2000), Fungi as geological agents, *Geomicrobiol. J.*, *17*, 97–124.
- Tudhope, A. W., and M. J. Risk (1985), Rate of dissolution of carbonate sediments by microboring organisms, Davies Reef, Australia, *J. Sed. Petrol.*, *55*, 440–447.
- Verrecchia, E. P. (2000), Fungi and sediments, in *Microbial Sediments*, edited by R. E. Riding and S. M. Awramik, pp. 68–75, Springer, New York.
- Verrecchia, E. P., J. L. Dumont, and K. E. Verrecchia (1993), Role of calcium oxalates biomineralization by fungi in the formation of calcrites: A case study from Nazareth, Israel, *J. Sed. Geol.*, *63*, 1000–1006.
- Vogel, K., M. Gektidis, S. Golubic, W. E. Kiene, and G. Radtke (2000), Experimental studies on microbial bioerosion at Lee Stocking Island, Bahamas and One Tree Island, Great Barrier Reef, Australia: Implications for paleoecological reconstructions, *Lethaia*, *33*, 190–204.
- Warscheid, T., and J. Braams (2000), Biodeterioration of stone: a review, *Int. Biodeterior. Biodegrad.*, *46*, 343–368.

Wilson, M. J., and P. Bayliss (1987), Mineral nomenclature: Glushinskite, *Miner. Mag.*, 51, 327.

Wilson, M. J., D. Jones, and J. D. Russel (1980), Glushinskite a naturally occurring magnesium oxalate, *Miner. Mag.*, 43, 837–840.

Wright, P. (1986), The role of fungal biomineralization in the formation of Early Carboniferous soil fabrics, *Sedimentology*, 33, 831–838.

---

P. Claeys, E. Keppens, and K. Kolo, Department of Geology, Vrije Universiteit Brussel, Pleinlaan 2, Brussels, B-1050, Belgium. (phclaeys@vub.ac.be; ekeppens@vub.ac.be; kamal.kolo@vub.ac.be)

A. Pr eat, Universit  Libre de Bruxelles, D partement des Sciences de la Terre et de l'Environnement, CP 160/02, 50 Av. FD Roosevelt, Brussels, B-1050, Belgium. (apreat@ulb.ac.be)